Stony Brook University

Identification of Process Conditions and Stress Evolution in Thermal Spray by Detailed Simulation

A Thesis Presented

by

Shu Guo

to

The Graduate School

in Partial Fulfillment of the

Requirements

for the Degree of

Master of Science

in

Mechanical Engineering

Stony Brook University

August 2010

Stony Brook University

The Graduate School

Shu Guo

We, the thesis committee for the above candidate for the

Master of Science degree, hereby recommend

acceptance of this thesis.

Toshio Nakamura – Thesis Advisor
Professor – Department of Mechanical Engineering

Chad Korach – Chairperson of Defense
Assistant Professor – Department of Mechanical Engineering

Sanjay Sampath – Outside Member
Professor – Department of Materials Science and Engineering

This thesis is accepted by the Graduate School

Lawrence Martin
Dean of the Graduate School

Abstract of the Thesis

Identification of Process Conditions and Stress Evolution in Thermal Spray by Detailed Simulation

by

Shu Guo

Master of Science

In

Mechanical Engineering

Stony Brook University

2010

Thermal sprayed Yttria stabilized Zirconia coatings are fabricated with melted or semi-melted particles solidifying on substrates. This process results in the unique layered, porous and cracked morphology of thermal sprayed ceramic materials. Meanwhile, the stresses within coatings evolve throughout fabrication process. During the actual experiments, the conditions, such as preheat temperature of substrate, raster speed as well as feed rate can influence the stress evolution and residue stress. To quantifying the influences of these associate process conditions, a very detail simulation method of thermal spray is employed in this paper.

To exhibit the simulation, nonlinear material properties are to be identified from experiments. First, a suitable stress-strain model is introduced, following by a nonlinear bi-material beam solution. Afterward, an inverse analysis procedure is introduced to process curvature-temperature measurements to extract unknown parameters. With the material properties and input the process condition, a detail simulation is carried out corresponding to the experiments. From the simulation, the temperature at the bottom of substrate and curvature measurements through ICP can be replicated to validate the result

of simulation. After the verification of the simulation, the influence of preheated temperature, raster speed and feed rate is studied separately. Moreover, experiments will be implemented to verify these conditions' influence.

The stress evolution can reveal the information of coating formation and properties. From the simulation, this becomes very easy and obvious comparing with experiments. Also, the residue stress can be obtained directly from the simulation. In the end, to validate the prediction of simulation, experiments are carried out to compare with the results obtain from simulation.

To my parents and friends

For their supports

Table of Contents

List of Figures ..... **viii**

List of Tables ..... **xi**

1. Introduction **1**

2. Identification of nonlinear property **3**

2.1 Constitutive model 3

2.2 Nonlinear Bimaterial Beam Solution and Unknown Parameters Estimate 4

3. Detailed simulation of spray deposition process **6**

3.1 Method introduction 6

3.2 Geometrical model 7

3.3 Material properties 8

3.4 Thermal and Heat Flow Conditions 8

3.4.1 Heat input 9

3.4.2 Heat output 10

3.4.3 Thermal condition settings in deposition process 10

3.5 Simulation Sample with Curvature-Temperature Measurements 11

3.5.1 Sample parameters settings 11

3.5.2 Measurements of Curvature and Temperature 12

4. Comparison Study with Experiments **13**

4.1 Sample Implementation 13

4.2 Other Simulation Results 15

4.3 Discussion of simulated results 17

4.3.1 Parameters in simulations setup considering feed rate and raster speed 17

4.3.2 Residual stress 19

4.3.3 Stress evolution 20

4.3.4 Conclusion and other phenomena 21

5. Effects of variant parameters 22

5.1 Effect of Preheat Temperature 22

5.2 Effect of thermal parameters 23

5.2.1 Effect of heat input 23

5.2.2 Effect of heat output 23

5.3 Effect of material properties 24

5.3.1 Young's modulus of coating 24

5.3.2 Substrate properties 25

6. Conclusion 26

References 28

Appendix 30

List of Figures

Figure 1. Nonlinear stress-strain relation model for TS ceramic coatings. Change in linear and nonlinear stress-strain relation occurs at transitional stress σ_T. Corresponding equations are noted below and above the ε^* axis, respectively. 31

Figure 2. Schematic of TS coating on substrate with relevant dimensions. Corresponding material parameters are noted and the location of neutral axis y_o is shown. 32

Figure 3. Flowchart to compute curvature change $\Delta\kappa$ for a given moment change ΔT... 33

Figure 4. Finite element model of YSZ coating beam. 26700 elements are used in the model. Smaller elements are required for coatings to simulate the nonlinear properties and avoid inconsistent results in stress and strain. 34

Figure 5. Simulated curvature and temperature results from simulation with high deposition temperature but no heat energy input. 35

Figure 6. Temperature field distribution of new added nodes in certain deposition job. 36

Figure 7. Accurate simulation of thermal spray deposition process through adding elements along transverse direction under proper heat transfer. The bottom figure shows cool down of completed deposition. 37

Figure 8. Schematic of curvature change as coating and substrate is thermally sprayed and thermal cycled. ICP sensor in placed at the bottom of substrate. Three points of measurements report the curvature change throughout the deposition process and cooling down process. 38

Figure 9. Simulated (a) temperature and (b) curvature results from simulation. For comparison experimental results are also shown. Magnified curves in insets have different coordinate scales. 39

Figure 10. Schematic figure of stress within the specimen. The tension is defined as positive value. The compression is defined as minus value. The deform is derived from

the bending caused by different CTE (coefficient thermal expansion) during deposition process..... 40

Figure 11. Comparison between experiment and simulation of (a) temperature and (b) curvature results of experiment R918. The red line stands for the simulation results. As (a) shows, the simulation takes longer time to reach the steady state. While the value of temperature fits well. In (b), the curvature of simulation has less oscillation. 41

Figure 12. Raster path in TS deposition process vs. simulation. The simulation adopts two dimensional model, which cannot present lattice path style in experiments. 42

Figure 13. Comparison between experiment and simulation of (a) temperature and (b) curvature results of experiment R920. Better match results due longer deposition time. 43

Figure 14. Comparison between experiment and simulation of (a) temperature and (b) curvature results of experiment R922. Due to small difference of steady state temperature and preheat temperature, the simulation reach the steady state quickly. 44

Figure 15. Raster path of experiment. The lattice paths are raster path of nozzle. The red rectangle is sample, fixed by four dots. There are extra path of raster other than on the specimen. 45

Figure 16. Residual stress through thickness of specimens. Left side of the dash line are substrates, the right side are coatings. Zero marks the interface. 46

Figure 17. Stress evolution during the deposition process and residual stress after cooling down within YSZ coating of R918. Zero of x axis means the interface with substrate. Four moment of deposition process (120 sec, 240 sec 360 sec and 480 sec) are recorded. The dash line remarks the interface of tensile stress and compressive stress. 47

Figure 18. Quenching stress and residual stress within specimen of R918. Zero of x axis means the interface of coating and substrate. The left side is substrate, the right side is coating. 48

Figure 19. Coating residual stress profile of R918 after cooling down. 49

Figure 20. Different preheat temperature simulation comparing the simulation of specimen R920. 50

Figure 21. Different heat input values of simulations comparing the simulation of specimen R920. 51

Figure 22. Schematic model of convection condition in deposition process as well as cooling down process. 52

Figure 23. Different heat output values of simulations comparing the simulation of specimen. 53

Figure 24. Trial simulation with different value of linear properties in coating. 54

Figure 25. Deposition simulation with different value of conductivity of substrate. 55

Figure 26. Deposition simulation with different value of specific heat of substrate. 56

List of Tables

Table 1. Basic parameters of specimens' simulations carried out to match the experiment. These values can be obtained directly through the experiment data except for the heat flux value in the last column. 57

Table 2. Thickness of path and steady state temperature of four specimen experiments. Tst Stands for the temperature achieved in steady state. 57

Acknowledgements

The two years' study in pursuing a master degree is the best experience of my life. I am deeply grateful to my advisor, Professor Toshio Nakamura. His broad knowledge and passion toward scientific research encourage me to devote myself to the study of solid mechanics. He is not only a mentor on academics but also with a concern for the well being of his students. Besides my advisor, I also want to thank the rest of my thesis committee, Professor Chad Korach and Professor Sanjay Sampath, who gave me insightful comments and reviewed my work on a very shot of notice. Special thanks to Gopal Dwivedi, Dr. Shinoda Kentaro, Alfredo Valarezo and Dr. Yang Tan from Department of Materials Science and Engineering. They helped me with the knowledge of thermal spray and gave lots of advice on my thesis.

I am indebted to my senior colleagues: Dr. Yajie Liu, Xi Yang and Chong Huang for their generous help. I also want to thank all my fellow group colleagues: Jiandong Yu, Changhong Cao, Zhiyun Li, Yu Chen, Wei Zhao and many others, for their care, support and friendship. I would also like to thank all the faculty and staff in the Department of Mechanical Engineering, for their help with my studies and financial support from NSF GOALI-FRG program under award CMMI 0605704.

Last but not the least, I want to thank my beloved Seven and my parents, for their loving, supporting, concerning and understanding during my graduate study. This thesis is dedicated to them.

To all of you, thank you.

1. Introduction

Thermal sprayed (TS) coatings are widely used in Aerospace, automotive, biomedical, paper making, oil and gas, electronics, and food processing equipment. This technique is extremely effective in increasing component life and value, decreasing machinery down-time, and improving performance in a wide variety of applications. As the engineering application increases, their mechanical reliability becomes more critical to ensure designed performances. The coating's properties, such as effective modulus, thermal conductivity and residual stresses, are key factors in understanding coating's reliability (Kesler et al., 1998). Moreover, with the spread application in industries, mass production is need in many circumstances. Thus, the repeatability is more crucial than any other factors else.

Traditionally, TS ceramic coatings are synthesized with plasma spray guns where feedstock particles are melted at high temperatures. The molten or semi-molten particles hit on the substrate and solidify rapidly to form a coating on substrate. This process generates lamellar microstructure as well as many defects within the specimen. This structure results in the nonlinear mechanical elastic behavior when the micro-cracks and pores and sliding between splats interfaces open or close the under compressive and tensile load (Liu and Nakamura, 2006). In detail, when high compressive load applies to specimen, crack faces are closed and the coatings exhibit higher apparent stiffness while opened cracks under tensile state produce more compliant response (Kroupa and Dubsky, 1999; Kroupa and Plesek, 2002). Many methods were carried out to exam the nonlinear properties of TS coating. Liu and Nakamura (2006) reported the nonlinear behavior of the thermal under thermal cycling test. Harok and Neufuss (2001) reported nonlinear behavior of atmospheric plasma sprayed (APS) $ZrSiO_4$ under four-point-bend tests. Waki et al. (2004) observed the nonlinear stress-strain responses of plasma sprayed zirconia coating using the laser speckle strain-displacement gauge (SSDG). Wang et al. (2006) showed nonlinear stress-strain relation of thermally sprayed metallic Ni–45Cr coating under tensile loading along the through-thickness direction due to its lamellar features.

The determination of the nonlinear property is important to evaluate effectiveness of the thermal spray coating. Kroupa and co-workers Kroupa (1999, 2002) built physical

models relating theoretical defect geometries to macroscopic non-linear mechanical response. Liu and Nakamura (2006) provided an effective method to estimate the nonlinear properties of the TS coating under thermal cycling test. This research sets a very precise model and determines the properties of coating in a very detailed way.

More important in TS process is to study all affect factors to the nature of the deposit formation dynamics and the ensuing properties of coatings. And also it turns out that such studies are extremely useful for achieving the repeatability of coating fabrication and the reliability process system. So, accordingly, architecture of the coating thus strongly related to the complex deposition processes and related processing conditions are investigated (Brinkiene et al., 2004; Deshpande et al., 2004; Friis et al., 2001; Kadolkar et al., 2002, 2003; Kweh et al., 2000; Li et al., 2003; Mawdsley et al., 2001; Montavon et al., 1997; Ning et al., 2006; Sampath et al., 2004; Teixeira et al., 1999; Thangamani et al., 2002; Zhao et al., 2004). During the research, the actual TS process is not easy to set up. And due to many parameters in experiments, repeat the TS process is hard to achieve. Comparing other auxiliary tools, simulation provides a vivid method which can record the process and repeat the process in much easier way. Also, by setting up different parameters in simulations, experiments can be investigated in a more detailed ways.

In this paper, a very detailed simulation is constructed according to actual thermal spray process of yttria stabilized zirconia (YSZ) coatings. To validate the simulation, several experiments are matched by investigate the temperature and curvature measurements. After that, the simulation is discussed by the parameters which would affect the stress or other properties.

2. Identification of nonlinear property

2.1 Constitutive model

In order to describe the coating's nonlinear behavior, a phenomenological constitutive model is introduced (Nakamura and Liu, 2007). First, based on the experimental observations and likely physical causes of nonlinearity (cracks and defects), the stress-strain relation should be asymmetrical under compression and tension. Second, under very large compression, the response should be nearly linear since many cracks and thin defects are closed. Thirdly, the transitional point from linear to nonlinear generally does not occur at zero stress (σ = 0). Since the experimental data suggest continues change of the coating stiffness, the following uniaxial stress-strain model is proposed:

$$\varepsilon = \begin{cases} \dfrac{\sigma}{E} - \dfrac{\left|\sigma_T\right|^n}{E\sigma_N^{n-1}} & \text{for} \quad \sigma < \sigma_T \\ \dfrac{\sigma}{E} + \dfrac{(\sigma-\sigma_T)^n - \left|\sigma_T\right|^n}{E\sigma_N^{n-1}} & \text{for} \quad \sigma \geq \sigma_T \end{cases} \tag{1}$$

Here, E is the elastic tangential modulus under small applied moment, n is the power-law exponent and σ_N is the reference stress. Also σ_T is the transitional stress where coating behavior changes from linear to nonlinear. Generally it is negative ($\sigma_T < 0$). The tension part of the model represents a combination of the linear elastic model and a modified Ramberg–Osgood model, if the transition is assumed to occur at $\sigma_T = 0$.

Figure 1 shows a schematic stress-strain relationship according to the (1). The stress-strain axes (σ^* - ε^*) centered at $\sigma = \sigma_T$ separates the linear and non-linear regimes. This model can describe many kinds of stress-strain behavior of TS coating with just four parameters (E_C, n, σ_N and σ_T). Also note E is appropriately described as the elastic tangent modulus near room temperature since it is not the modulus at σ = 0. The presented stress-strain model has been demonstrated suitable to describe the non-linear behavior of TS coating by many experimental data and previous jobs of T. Nakamura and Y. Liu. Although more precise description may represent TS coatings, they would require more parameters thus more computational burden.

2.2 Nonlinear Bimaterial Beam Solution and Unknown Parameters Estimate

To represent the behavior of coating and substrate system, the formulation for nonlinear bimaterial beam solution is described here. Although this procedure is straightforward, the derivation of it is rather complicated due to the shift of the neutral axes of the coating as the stress changes (Liu and Nakamura, 2006). Furthermore, although there have been studies on large deformation effects on beams and plates (e.g., Finot and Suresh, 1996), a complete solution for the nonlinear elastic bi-material beams is fairly difficult to find out.

Suppose a bimaterial specimen consists of a nonlinear elastic coating and linear elastic substrate as shown in Figure 2. Due to the mismatch of CTE (the coefficient of thermal expansion), the bimaterial specimen would bend to equilibrate thermal expansions of coating and substrate. In linear case, the curvature change during spraying and cooling can be expressed as (Tsui and Clyne, 1997)

$$\Delta\kappa = \frac{6E_s E_c ht(h+t)\Delta\alpha\Delta T}{E_s{}^2h^4 + E_c{}^2t^4 + 2E_s E_c ht\left(2h^2 + 3ht + 2t^2\right)} \qquad (2)$$

Unlike the linear elastic coatings, the neutral axis shifts with change in the secant modulus. The curvature change relates to the moment as $\Delta\kappa = M_{mis}/(EI)_{\text{bimaterial}}$. Here M_{mis} (per thickness) is generated by the mismatch force F_{mis} needed to equilibrate thermal expansions of coating and substrate. $(EI)_{\text{bimaterial}}$ is the effective flexural composite stiffness which varies with the neutral axis and the secant modulus. With these relations, a reduced iteration loops is assumed the following form (Liu and Nakamura, 2006),

$$\Delta\kappa \cong \frac{6E_s E^*_{ave} h\ t(h+t)\Delta\alpha\Delta T}{E_s{}^2h^4 + E^*_{ave}{}^2t^4 + 2E_s E^*_{ave} h\ t\left(2h^2 + 3ht + 2t^2\right)}. \qquad (3)$$

Here $\Delta\kappa$ is the curvature change under temperature variation ΔT, $\Delta\alpha = \alpha_s - \alpha_c$ and E^*_{ave} is introduced as the average secant modulus through thickness of the coating. E_s and h are the Young's modulus and thickness of substrate, respectively, t is the coating.

To further reduce the computational requirement, instead of computing the correct average value, E^*_{ave} can be estimated at the midpoint of coating ($y = h + t/2$) as,

$$E^*_{ave} \cong \frac{\sigma(\varepsilon_c^{\,mid})}{\varepsilon_c^{\,mid}} \quad \text{where} \quad \varepsilon_c^{\,mid} = -\Delta\kappa\left(h + \frac{t}{2} - y_o\right) + \frac{E_s h}{E_s h + E^*_{ave} t}\Delta\alpha\Delta T \quad (4)$$

Clearly, the computation of E^*_{ave} still requires multiple iterations. The curvature formula (3) for the nonlinear beam appears to be similar to the one given for the linear elastic case (2).

However, the required computations are very different and the determination of unknown material properties for a given $\Delta\kappa$–ΔT record is not a simple process. In the previous work, a procedure to calculate curvature for a given temperature change ΔT is developed, the flowchart is shown in Figure 3.

Furthermore, in order to determine the nonlinear coating properties, the constitutive equation (3.1) has four parameters E_c, σ_N, n and σ_T to be defined. To estimate them, an inverse analysis utilizes the Kalman filter technique (Kalman, 1960, Nakamura et. al., 2000, Gu et. al., 2003, Vaddadi et. al., 2003, Nakamura and Liu, 2007) to estimate the reference stress σ_N and the power-law exponent n.

With determined those parameters to describe material properties, a program to re-generate the schematic stress-strain relationship as shown in Figure 1 will be employed (attached in the Appendix). Throughout this program, a code for Finite Element Analysis software will be output. By this work, the simulation will precisely replicate the experimental procedure by using the actual properties of coating.

3. Detailed simulation of spray deposition process

In the previous chapter, non-linear mechanical properties of TS YSZ coatings are identified. Simulation is a powerful verification of it. Furthermore, simulation can be very good guide to predict experiment result. With the non-linear mechanical properties of coatings as prerequisite, we can perform duplicate simulation comparing with experiment. To set up successful simulation, experiments environment must be investigated carefully and represented as suitable boundary conditions in simulation. In this chapter, the simulation procedures are introduced carefully. However, certain simulation results are discussed later because they need to be matched with certain experiments.

3.1 Method introduction

Thermal Spray is a widely used industry method to improve materials properties. But there are rarely simulation work accomplished about it. Similar works have been carried out by Bengtsson (1997), Lugscheider (2003) and Ghafouri-Azar (2005), etc.

To obtain full computational result of thermal cycle, there are two major parts of simulation. One is to simulate TS deposition process, the other one is cooling down period. Deposition part is much more complex than the latter one. To reduce computational burden while keep accuracy of simulation, a two-dimension model is implemented. Elements are built up along both horizontal and vertical directions to reproduce the process of deposition of YSZ coating by characterize continuous depositions of YSZ layers. This complex simulation shows the essence of the thermal spraying experiment.

General commercial finite element software cannot generate new nodes and elements in a certain job. In order to accomplish this idea, a program utilizing C language is employed (which is attached in the Appendix). In this program, nodes and elements are generated into text file in certain format. Moreover, input file for each job is generated either, which contains the geometrical model, material properties as well as boundary conditions, etc. When the simulation is carried out, the program can assort the files of nodes and elements with input file, then submit the input file to computers.

After deposition process, the model exposes to an environment forced air convection. This part does not need re-mesh of the geometrical model and the settings are very straight forward. So the following of this chapter will focus on key issues to simulation of deposition process.

3.2 Geometrical model

The YSZ coating is fabricated on the substrate. So the simulation starts with the geometrical model of the substrate. It is assumed to be aluminum, whose elastic modulus is changed with temperature. The thickness of substrate is set to be h = 3.2mm, the length is 40mm. Although the length is shorter than actual specimens, it is still large enough compared to the thicknesses. To obtain more accurate analysis results, the elements are set to be thinner by thinner when approaching the top layer.

In the actual TS process, a plasma gun is moved transversely to deposit molten particles. At each pass, the coating deposition is simulated by adding five layers of elements. To simulation accurately, a special care was taken to reproduce the actual deposition. Since the spray gun deposition rate varies with radial distance (more near the center), the element addition was carried out as a moving inclined slope. The sizes of elements were chosen carefully to optimize the accuracy and computation time. Among the five layers, the first one and the fifth one is thinnest and they are equal to each other. The second and fourth layer is thicker than them. And the third one is the thickest. The finite element model of substrate and coating is partly shown in figure 4.

Based on different samples of fabrication process, the number of passage and the thickness of each layer are better to be set as variable. So they can change to match different experiments. This means the final thickness of YSZ coating can be changed, either.

In total, 2,400 elements are used for the substrate. And for coating, it can be change as required. However, a significant amount of computational time was required to carry this simulation since the total number of re-meshing was huge. From the algorithm developed to generate new nodes and elements, each passage includes 64 jobs. So the re-mesh times and coating elements number is dominated by the number of passage.

3.3 Material properties

In usual experiments, the substrate remains aluminum plate. This is because YSZ tend to bond well to the aluminum substrate and the high thermal conductivity of aluminum also reduced propensity for thermal gradients in the substrate. Since the properties of aluminum are sensitive to temperature change, the Young's modulus and the coefficient of thermal expansion flow are modeled as temperature dependent (Material Properties Database, 1999),

$$\begin{aligned} E_s(T) &= -2.65\times10^{-7}T^3 + 2.4\times10^{-4}T^2 - 9.21\times10^{-2}T + 85.2 \text{ (GPa) for } 113\text{K} < T \le 573\text{K} \\ \alpha_s(T) &= -9.27\times10^{-12}T^2 + 2.59\times10^{-8}T + 1.54\times10^{-5} \quad \text{(1/K) for } 283\text{K} < T \le 575\text{K} \end{aligned} \tag{5}$$

The temperatures ranges are chosen in relevant to the present tests. Although in the experiments, the high temperature reaches only up to ~250^{o}C (523K) or a little even higher, the inclusion of temperature dependent properties for aluminum is very important in the estimations. Furthermore, plastic flow of the aluminum was not considered although limited yielding probably occurs when the substrate is struck with molten particles since the stress in substrate is not very high. The other parameters for the aluminum were chosen as ν = 0.33, ρ = 2,702Kg/m^3, thermal conductivity K_{Al} = 155W/m·K and specific heat capacity c_{Al} = 963J/kg·K.

As for the coating, the mechanical property was assumed to follow the nonlinear relation shown in figure 1. In the simulation carried out here, the parameters of E_c, ν, σ_0, n, σ_T, T_T are need. This is implemented by certain subroutine in simulation. Other parameters include the mass density ρ = 5,436 Kg/m^3, the thermal conductivity K_{YSZ} = 1.0 W/m·K and the specific heat capacity c_{YSZ} = 360J/kg·K remain the same in all simulations. All of above characterize the properties of YSZ coatings demanded of simulation.

3.4 Thermal and Heat Flow Conditions

After complete the algorithm to generate nodes and elements, the boundary condition is to be considered. To simulate actual TS process, there is no mechanical loading. So to represent the process as closely as possible, thermal and heat flow conditions must be set very carefully and reasonably.

3.4.1 Heat input

The new elements are added to replicate the process of TS coating materials hitting the top surface. As described before, the simulation is constituted by amount of jobs, means many times of re-mesh. As discussed before, the number of re-mesh is determined by the number of passage. In a certain job of simulation, newly added elements and nodes do not have successive temperature information from the previous job. Thus, the temperature of new nodes is 0°C. So in order to keep new nodes and elements are hotter than the existing model, the temperature level should be shift down. In other words, if the temperature of new nodes is 500°C, in order to remain temperature around the model as 25°C, the environment temperature should be set -475°C in the simulation. As the consequence, the aluminum property, which is temperature dependent, is to be changed by minus 500°C from the temperature values.

But merely keep newly added nodes at higher temperature is not enough. A test simulation is carried out. When the temperature of new nodes is set to be 3000°C, very severe deformation is observed from the curvature shown in figure 5 (a). But the temperature monitored at the bottom of the substrate keep dropping to as low as around 80°C, as shown in figure 5 (b). Furthermore, for a new element, only two nodes on top are newly added with 0°C, the other two nodes success the temperature information in the previous job to form a nonuniform temperature distribution within the element. In this case, we cannot satisfy the whole element to be uniformly 0°C. This situation is stated in figure 6.

Apparently, in actual experiment, the deformation is not thus significant. In the meanwhile, the solidified drops do not have such high temperature. In fact, to replicate the TS process, energy input from the solidified drops must be taken into consideration. So, in the simulation the environment temperature is set to be -475°C, which means the nodes added are 500°C. This is because although molten particles have much higher temperature, as soon as they strike the plate, the temperature drops immediately. As discussed before, heat flux is needed through new nodes. The heat flux was chosen to be q_{in} , which can be changed with different samples of experiment. There will be continuous heat energy input by this manner.

3.4.2 Heat output

During the deposition and cooling down periods, the heat is continuously taken away by forced air convection while deposited molten particles add heat to the specimen. In this simulation, only bottom of the substrate and top of the model except for new elements are taken into considered into output setting. The left and right sides are not included because of the limited area of them and simplification of program. The heat flux out of surfaces was modeled with the following equation.

$$q_{out} = h(T - T_{\infty}) \quad (6)$$

Here h is heat transfer coefficient. It is to be chosen carefully corresponding to the value of q_{in}. These two parameters determine the temperature monitored. The method is to find h first due to match of cooling down period. Because this period does not involve heat input. After h is chosen, since all tests are conducted at the same locations under similar conditions, this parameter is fixed for all deposition and cool down simulations. The heat input through the molten particles is chosen by comparing the simulated and measured temperature records.

T_{∞} is ambient temperature and T is the surface temperature. According to the setting of environment temperature, T_{∞} equals to actual ambient temperature minus expected temperature value of new nodes. After simulation, the temperature gathered must add to expected temperature value of new nodes, too. The heat flow conditions are illustrated in figure 7.

3.4.3 Thermal condition settings in deposition process

As discussed in 3.1, the cooling down period is very easy to simulate comparing to deposition process. In fact, except for the algorithm to generate new nodes and elements and setting of heat output from undefined top elements, the relationship of heat input and heat output within a certain deposition simulation job is worth investigating carefully. One obvious phenomenon in experiments is the oscillatory behavior during deposition in both temperature and curvature measurements. Figure 8 shows this clearly. This comes from the movement of plasma gun. It stops for a while after a spray action. When the gun stops, it means no heat input during that period of time. To repeat this

phenomenon in simulation, in each single job, heat input cannot go through the entire time of period. So, a concept of spray time and hold time is generated. In a single job, the time is split into those two parts equally. In spray time, the heat input and output are both active. While in the hold time, there is only heat output. In this way, the oscillation can be reproduced as the experiments shows.

3.5 Simulation Sample with Curvature-Temperature Measurements

As introduced above, the simulation is completed in setting. Firstly, the substrate is pre-heated to a certain value. Then run the program with all parameters ready, the model is to re-mesh to replicate deposition process and carried out simulation automatically. After that, the cooling down period is to simulate until the model reach the ambient temperature.

3.5.1 Sample parameters settings

In the previous part, there are some parameters that remain the same all through this paper. As for substrate, the geometrical model, the material properties are set. Besides, some of the coating properties as density, thermal conductivity and specific heat capacity remain same. And the heat transfer coefficient of heat output does not changed either. Here a sample of simulation is taken out. The parameters are trial for a glancing investigation.

Following the introduction above, the geometrical model is to be set firstly. Despite the substrate, the coating thickness is t = 277μm including 15 passages. Each passage is 18.5μm with five layers elements.

As for the coating, nonlinear relation is constituted by E_c = 22.8GPa, ν = 0.32, σ_0 = 38MPa, n = 2.65, σ_T = –22.1MPa at T_T = 30°C.

In thermal and heat transfer condition, the heat output employs h = 45W/m^2·K in (6). While the heat input is defined by heat flux q_{in} = 210W/m^2. To generate oscillation, the spray time and hold time are equal to each other.

3.5.2 Measurements of Curvature and Temperature

The finite element analysis was carried out under transient coupled heat-transfer and stress condition. The temperature is obtained at the mid-point on the bottom surface as in the actual tests where a thermo-couple attached to the substrate bottom is used. And ICP (Insitu Coating Property Sensor) is responsible for curvature measurements, figure 8 shows the installation of sensors and the curvature change as coating and substrate during thermally sprayed and thermal cycled. To represent the curvature in value, the tension is defined as positive value and in the contrary the compression of sample is defined as minus, like figure 9 shows. In simulation, three points' displacements are record to compute the curvature. Among these three, the two by the side are fixed, so only the node in the middle is needed for curvature result.

The results of temperature-curvature measurements are shown in figure 10. The oscillatory behavior during deposition in both temperature and curvature experimental measurements are accurately captured in the computational simulations.

After 4~5 spray passes, the substrate temperature appears to reach the steady state. This suggests the heat input from particles and the heat removed from the specimen are approximately equilibrated. Since new elements added to the substrate have high temperature and they immediately cool down, the state of stress in the coating is tensile. These stresses cause the curvature to increase during the deposition as shown in figure 10. After the deposition is completed at t = 190sec, both substrate and coating immediately cools down (from 246^{o}C to 20^{o}C). During the cool down phase, the same heat transfer coefficient h = 45W/m^{2}·K in (6) was imposed across the substrate and coating surfaces. Since the CTE of substrate is higher than that of coating, the curvature reverses its sign and it eventually makes the overall stress in the coating to be compressive.

4. Comparison Study with Experiments

In the previous chapter, the simulation procedures are introduced in detail. In order to further study how the parameters in the experiments affect the properties of coatings, the simulation must be proved to be valid firstly. In order to do this, certain experiments are employed for comparison. The material properties are determined by the inverse analysis. Then it is used in simulation. By investigating the temperature of the middle position at bottom and the curvature change of the substrate, values of some key parameters are determined.

4.1 Sample Implementation

Unlike the previously sample study in chapter 3, this time real experiments are to be replicated. The criterion of choosing experiments is that the longer deposition lasts the better. Because as shown before, the temperature measured in experiments will reach steady state. Thus, in order to eliminate error and replicate the steady state more precisely, longer steady state period is needed. Among the existing experiments, R918, R920 and R922 are chosen. In table 1, the information such as raster speed, feed rate, and thickness of coating per pass are shown by actual specimen number. Although three experiments are to be cited in matching with the simulation, in this section, however, only R918 will be replicate in simulation to show the procedures meticulously. The results of other experiments will be introduced later.

As described in section 3.5.2, a thermo-couple attached to the substrate bottom is used to monitor the temperature in the middle position of the bottom. And ICP is employed to record the curvature information. The temperature and curvature record in the simulation will truly reproduced as did in experiments.

Also, Al6061 substrate was chosen as the substrate material. There were several reasons for this. Primarily, aluminum provided significant deflection, due to relatively low stiffness, and high thermal mismatch with YSZ, for high fidelity curvature measurements which would allow careful extraction of nonlinear parameters in thick top coats (Nakamura and Liu, 2007). Because YSZ tended to bond well to the aluminum

substrate and the high thermal conductivity of aluminum also reduced propensity for thermal gradients in the substrate, but bonded poorly to the steel and resulted in delamination. The equation (5) shows that the Young's modulus and the coefficient of thermal expansion of substrate are modeled as temperature dependent.

As discussed in Chapter 2, the nonlinear YSZ coating properties are generated from inverse analysis of Kalman Filter. E_c, ν, σ_0 and compression or tension condition are chosen to represent the properties in subroutine in FEA software. Using these parameters, the stress-strain relation is reconstructed as shown in figure 1. Essentially, the slopes outside these bounds are extrapolated results since only the records between these temperatures are actually used to estimate the property. Note the coating may behave in a different way outside the range, especially under large tensile load (e.g., further cracking). A computational code generates the stress and corresponding scant modulus to represent the nonlinear relationship. This is needed in the simulation to guarantee the replication.

As shown in figure 11, R918 has 20 passes of raster. Here in simulation, the preheat passes are ignored because the substrate is heated directly as the initial condition. And the curvature would be set as zero when the preheat takes place.

To replicate the simulation, the most important parameters are thermal parameters. In simulation, they are heat input flux and heat transfer coefficient h. In order to determine them, we have to consider one of them each time, because the results depend on both of them. Note here we consider the cooling step first. As stated in chapter 3, the cooling step only needs the heat coefficient h. The model here should be the specimen after the spray process, which means the coating is attached with the substrate. What is more, the initial temperature should be set as the steady state of the experiment. In simulation carried out, h of the bottom as well as the top should be same, it is determined to be h = 40W/m^2·K. With this value, the curvature and temperature figures of cooling down simulation can be precisely fit with those in experiment.

After this, we have to setup other useful parameters. First, we have to determine the geometrical control parameters. The thickness of substrate is easy to set. According to the experiment information, the thickness of coating of each layer should be as 40.8μm, thus the total of 20 passes should be 0.898μm as indicated. Then, according to the experiment part of figure 11, the spray process takes about 500 seconds. So the spray

time and hold time can be determined either. The preheat temperature is 237.3°C. If 500°C of deposition temperature is considered, the value set in the input file is -262.7°C.

Next, several values of heat flux q_{in} are taken as trials. In order to fit the steady state temperature, it is set to be heat q_{in} = 300W/m^2. Read the temperature and curvature from the simulation, compare them with the experiment. The figure 11 shows the results.

From the comparison, it is obviously that the experiment takes less time to steady state temperature than the simulation. This is because the difference of simulation model vs. true spray process, as shown in figure 12. In simulation, 2D model is utilized, so the raster method is way different to the experiment one.

Moreover, from (a) in figure 11, the temperature of the simulation matches the experiment result good except the fluctuation in the simulation is not so great than the experiment. This phenomenon is because in the experiment, high velocity particles are striking onto to the substrate. Since such was not simulated, they were not observed in the finite element analysis.

4.2 Other Simulation Results

In this section, R920 and R922 are going to be replicated as done to R918. Some basic details have been introduced in table 1, moreover, the following figure 13 and figure 14 show the curvature and temperature change versus time of experiment R920 and R922 respectively.

According to the experiments' information, the thickness of coating of R920 and R922 is only 1/3 of that in R918. This render the heat input through the nodes may decrease. In this case, some adjustment of heat parameters should be carried out. The method to select new parameters is the same with what we did before in matching the simulation to experiment of R918. The value of heat coefficient h, thus, should be determined first and this value is assumed the same as it was set before. This is because these experiments are supposed to be carried out in the same environment. Verification by matching the curves of temperature and curvature change during cooling down with h = 40W/m^2·K prove the assumption.

For experiment R920, after several trial value of q_{in} tested and q_{in} = 260W/m^2 is determined which can match the experiment data. This identify that the thinner coating thickness of each layer would correspond to lower heat energy input which is pretty straightforward.

Comparing with R918, R920 has more passes of raster. Technically, the simulation will be more precise when matching with the steady state. This is proved by figure x. It shows the curvature and temperature verses time of simulation and experiment correspondingly. From the figure, it is obvious that in case R920, the simulation takes less time to achieve the steady state. And with the results, we can find out that less thickness of coating means less heat input throughout the spray process. But the thickness of coating is related to the raster speed as well as feed rate. This issue will be investigated further.

Another experiment to be matched is R922. The thickness of each layer in coating is nearly the same with that in experiments R920. According to the experiment process, the spray time in R922 is shorter than R920. Assume that heat input during the spray process is proportional to the total thickness of coating, and then these two experiments will receive the same amount of energy input. The only difference of these two is raster speed, which can be expressed as spray time and hold time in every job, when five new elements are added. The time period is shorter in R922 than that of R920. But, note the unit of heat flux is W/m^2, means the energy input value does not relate to time length. Then the heat from coating particles should be the same. The reason to explain this difference in heat input is in the experiment, heat is also brought from flames, which blow coating particles to the specimen. And lower raster speed will bring more heat from flames. Thus, in concept, simulation of R922 would identify smaller value of heat flux.

When determining the value of heat flux, fix heat output, q_{in} = 210W/m^2 is adopted. This proves the concept introduced above. The following figure shows the comparison between experiment and simulation of specimen R922.

4.3 Discussion of simulated results

As discussed above, the simulation matches the experiments very well when comparing the results of curvature and temperature measurements in experiments. In this case, it is suitable to use simulation results to do some research about thermal spray process. Furthermore, the simulation can provide many results such as transient stress fields, transient temperature field, or observe the stress through the coating layers which is hard to measure in experiments. This section will introduce some simulation result to explain relative phenomenon.

Three experiments have been picked out since they have long deposition process and they can be used to investigate the effects of feed rate and raster speed. But to cover all four combinations of high and low value in feed rate and raster speed, one more cases are needed here. From the raw date, R921 is the substitute for the vacancy. As shown in table 2, these four specimens are listed.

In the first section of this part, to identify the parameters needed in simulation of R921, the effects of feed rate and raster speed to the parameters in simulation would be discussed. This can reveal a guide to set comparisons simulation to certain experiment.

4.3.1 Parameters in simulations setup considering feed rate and raster speed

The feed rate and raster speed are very important factors in thermal spray deposition process. These values control the raster nozzle to fabricate coating. Thus to set suitable value of feed rate and raster speed is very crucial. In simulation, the raster speed can determine the deposition time of each single deposition job. Feed rate and raster speed is to determine the thickness of coating. And heat flux in simulation is also related to these two values. Table 2 shows the parameters in simulations of these specimens.

From it, we can conclude that same raster speed render same deposition job time. In simulation, each job has five new elements. If the raster speed is the same, the nozzle moves in a constant speed, which fixes the job time. But from the values of the deposition job time, for example, the specimens with 250 mm/s do not spray three times slower than the ones with 750 mm/s, although the multiple between them is the same. This is because of the setup of experiments. As shown in figure 15, the specimen is placed in the middle of the platform where spray takes place. The raster path is actually more than the length

of the specimen. Moreover, the nozzle needs to speed up and slow down in each single path. Considering these two reasons, the actual deposition time cannot be directly derived by relationship of raster speed. But according the simulation, when trying to generate simulations to compare different effects of raster speed, when the actual multiple is 3, the value of 1.667 can be referred to.

Other than deposition time of each job, the thickness of coating is determined by both feed rate and raster speed. In the case of same raster speed, the specimen with 45 g/min feed rate has roughly three times thickness of coating than that with 15 g/min, vice versa. Indeed, the thickness of coating can be identified by deposition rate, which involves feed rate and deposition rate. It can be illustrated as the efficiency of deposition. Among the specimens carried out here, R920 and R922 have the same deposition rate. As shown in table 1, the coating thickness is the same.

Also, the heat input value is related to the coating thickness as well as the raster speed as discussed in the last section. To find out the relationship of heat input with feed rate and raster speed, one of them should be fixed first. By the three simulation carried out, when raster speed is the same, for instance, R918 and R920, the heat input ratio between them is 300/260=1.154. It is suppose that when looking into R921 and R922, whose raster speed is 750 mm/s, the ratio equals to 1.154, either. So that when the raster speed is the same, increase of feed rate and improve the heat input by certain ratio.

By the investigation above, parameters of R921 are set without any trial or comparing with the actual experiment, as table 1 shows. The deposition job time is determined by the raster speed. It is set as the value of R922 since they have the same raster speed. The thickness is determined by the feed rate and raster speed by actually ratio. So the value is set as 0.0056 mm which is 1/3 of that of R920 and R922. As for the heat flux, the ratio 1.154 is applied with R922. It is determined as 182 W/m^2.

According to the experiment R921, this simulation needs 70 passes of coating, which cannot be modified since the aim to carry out the simulation is to match the experiment without any auxiliary trial. Although the simulation does not finished since the computational burden is too much. But the result is predicted to be valid since the temperature is examined in the middle of simulation, and the value is recorded very similar as the experiments.

With the analysis above, it can generate a guide to reproduce simulations without carrying out all experiments. In a simulation, there are only three parameters to be set if comparing different feed rate and raster speed. They are deposition job time, thickness of layer and heat flux, as shown in table 1. When one of them is carried out, by certain ratio of feed rate, the thickness of coating can be determined. Then, raster speed can fix the deposition job time.

4.3.2 Residual stress

Residual stress is a very important factor in thermal spray deposition. It can affects both processing and performance of coatings. High residual stress can lead to crack, delamination of coating, shape changes, etc. Thus, to understand it is very important. As discussed widely, the residual stress is originating from the large temperature differences, and results from two main contributions: quenching and thermal stress (cite the source). Quenching stress comes from rapid quenched particles hitting substrate in deposition process. It is tensile within coatings. And thermal stress is developed during cooling down process. The sum of these two stresses is residual stress. From simulation results, it is easy to find out the residual stress directly after cooling down to the room temperature. The effects of process parameters such as thickness of substrate, raster speed, feed rate, etc. will be discussed in the following chapter. However, through the cases taken out to match certain experiments, we can find out some roughly rules. Through our matching simulations before, refer to the table 2, R918 has low raster speed but high raster speed, R920 has low raster speed and low feed rate, and R922 has high raster speed and high feed rate. Figure 16 shows the residual stress versus thickness of specimen of these three cases of simulation.

In this figure, we can observe the oscillating of residual stress within coatings, but the same phenomena cannot be captured in the substrate. That may cause the delaminating within coatings are easier to form. Also, the significant gap of stress in the interface makes this position easy to fail.

R918 and R920 have the same raster speed. From figure 16, the higher feed rate renders higher residual stress. This is because higher feed rate brings in more heat and leads to larger temperature difference to form residual stress. In this same explanation,

raster speed contributes opposite as feed rate does. Higher raster speed will decrease the heat input from flames, thus make the residual stress less significant. Also, note that absolute value of residual stress in the coating of R918 is smaller than that of R920, although residual stress in substrate presents opposite. This is because R918 have thicker coating, thus when suffer same amount of moment of bending, the stress developed inside the coating would be less.

When comparing with R920 and R922, although they have different feed rate and raster speed, the deposition rate, which represent the efficiency of deposition, is the same. This can be illustrated by the same thickness of each single pass of coating. When refer to figure 16 above, with same deposition rate, the one with higher feed rate or lower raster speed would experience higher residual stress.

4.3.3 Stress evolution

Also, we can monitor the stress evolution during the deposition process. Figure 17 shows the stress development within coating of R918. From this figure, the stresses within the coating present a climbing trend during the process to approach the steady state. After reach the steady state, the stresses remain the same. The oscillation of stresses due to coating layers can be observed through deposition process either. And the stress drops down around 30 MPa because of cooling down process. This value can be referred as thermal stress as discussed before. Also, the stress change within substrate during the cooling down process can be shown either, in figure 17. The residual stress within coating has more significant oscillation between layers, cause the coating easier to delaminate.

Moreover, the quenching stress and residual stress can be calculated by simulation. Figure 18 shows the through-thickness profiles of quenching stress and residual stress. Although thermal stress cannot be shown directly, it can be calculate by the differences of those two. From the figure, the thermal stress should be very significant resulting from the large differences of residual stress and quenching stress. Since the thermal stress develops from the thermal mismatch of substrate and coating, we can conclude this specimen suffers large curvature drop during cooling down process.

4.3.4 Conclusion and other phenomena

In this chapter, the simulation is mainly an auxiliary tool to match with certain experiments. From matching with experiment, some basic concepts to identify the parameters in simulation are generated. The feed rate and raster speed, or the deposition rate controls the thickness of coating elements. The raster speed determine the deposition time. In the simulations carried out in this chapter, since the deposition time is limited by experiment, the effect of different raster speed does not bother much. Other than that, since the heat output is considered to be the same throughout the series of experiments, in order to match the simulations with experiments, the most important parameter to adjust is heat input. This value is relative to the thickness of coating, i.e. deposition rate, as well as the raster speed.

When the simulation is taken out, by comparing the temperature of middle point of bottom of substrate and the curvature change versus time, the simulations are matched by certain experiments. There are some differences since the actual thermal spray setup is different than that in simulation, such as the raster path, the dimension of model, etc. Still, the simulations can fit the experiments very well. Especially it provides power tool to investigate the stress evolution and the residual stress. Other than that, some transient fields can be observed either. For instance, figure 19 shows the high stress position of specimen of R918 after cooling down. From this figure, it is easy to predict the place with higher possibility to fail, which are the regions with higher stress. It is obvious that the first several layer and the both sides are easier to fail.

5. Effects of variant parameters

In the experiment, there are many parameters will affect the materials properties after deposition and cooling down process. Comparing with the inconvenience to repeat experiments, simulations provide a significant useful and powerful tool to investigate those effects. In this chapter, the parameter influence will be discussed quantitatively in detail. As the standard model, the simulation of specimen R922 is employed.

From the setup of the thermal spray experiments, many factors are to be considered. In the simulation, however, only should consider the preheat temperature of substrate, the heat input and output, as well as the substrate thickness as independent parameters. In the first section, the effect of preheat temperature would be discussed. Then, although in last chapter, the feed rate and raster speed in experiments are discussed. However, here the significance of heat input and heat output will be investigated. And at last, different substrate thickness will be taken into consideration.

5.1 Effect of Preheat Temperature

Refer to previous research work, preheat temperature can improve the coating integrity and adhesion. But most of them concentrate in the morphology of materials. In the simulation here, this cannot be investigated. But from general, by introducing different deposition and thermal environment, the effect of preheat temperature can be discussed.

The finite element analysis was carried out under coupled heat-transfer and stress condition. Figure 20 shows different preheat temperature cases of simulations. As mentioned, R922 is chosen as the standard simulation. In the control simulations, the only changed parameter is the preheat temperature. However, the curvatures of all cases remain zero when deposition starts.

From the comparison, although simulations start from the different preheats temperatures, the temperatures they reach at steady state is the same. Moreover, when investigating the curvature change, it is found that higher preheat temperature will lead lower increase of curvature during the deposition process. This means higher preheat

temperature can cause less stress within the specimen. Thus, higher preheat temperature can obtain more reliable coating.

5.2 Effect of thermal parameters

During the simulation setup in chapter 3, the thermal environment is discussed. There are two important parameters regarding thermal condition. One is heat flux, which represent the heat input energy, the other one is heat output value, indicating the convection condition of experiments. In this part, the heat input and heat output would be discussed respectively.

5.2.1 Effect of heat input

In the simulation carried out, heat fluxes are prescribed directly at node sets. It represents the heat energy concentration throughout the new elements to the existing model. In the comparison here, the only variable is heat input value. Thus, feed rate and raster speed are to be same during the simulations. If both of them remain unchanged, the only reasons to change heat input is the nozzle place, meaning whether it is nearer to the specimen or farther and the integrity of flame. So in some sense, to reproduce new experiment, heat input value can be fixed easily. This means repeatability of experiment is not so hard considering the heat input.

Figure 21 shows three cases with different heat input values. The difference between each adjacent case is 15 W/m^2. From the figure, the higher heat input would render higher increase of temperature value as well as the curvature value. But the curvature change is not that significant.

5.2.2 Effect of heat output

Other than the heat input, heat output is applied along the free surfaces of the specimen through elements. In simulation, the heat output is modeled as convection condition by air. Figure 22 shows the model.

The specimen is surrounded by flow of air. This model is governed by equation 7 to equation 9.

$$h = \frac{\overline{Nu}_L \cdot K}{L} \quad (7)$$

$$\overline{Nu}_L = C\,\mathrm{Re}_L^n\,\mathrm{Pr}^{1/3} \quad (8)$$

$$\mathrm{Re}_L = \frac{V_\infty L}{\upsilon} \quad (9)$$

Among the equations, Re_L is Reynolds Number, V_∞ is the velocity of the flow, which is shown in figure 22, L stands for the length of specimen. υ=15.89×10^{-6} m^2·sec as viscosity and K = 26.3×10^{-3} W/m·C. C = 0.1 ~ 0.3, is a constant. And Pr = 0.707, represents as Prandtl number. By the simulation trial, the value of h is fixed by 40 W/m^2·K. This means it is very possible that the heat output condition can remain unchanged in a series of experiments. In this case, repeatability cannot be achieved considering the heat output during the experiment.

Figure 23 shows three cases with different heat input values. The difference between each adjacent case is 5 W/m^2·K

5.3 Effect of material properties

In chapter 2, the nonlinear property for coating is established. In the simulation, the properties of material should be introduced at first, which means there is no way to predict material properties. But, some qualitative description can be illustrated from the simulation.

5.3.1 Young's modulus of coating

In this section, coating is assumed to be linear. This is only a simplified way to evaluate the modulus' influence in deposition process. As shown in figure 24, two simulations are carried out by modulus of 15GPa and 30GPa respectively.

From the comparison, the nonlinear properties nearly have nothing to do with temperature change. Two curve of temperature vs. time overlap with each other. However, the coating with lower modulus has smaller change of curvature during cooling down process, which means less deform to develop thermal stress.

5.3.2 Substrate properties

All simulations taken out in this thesis are using aluminum as substrate. However, some research of thermal spray use steel as substrate. In chapter 3 and chapter 4, some of the advantages of aluminum as substrate are listed. In this section, thermal conductivity and specific heat of substrate are to be investigated in simulations.

The simulations are only carried out in deposition part. The conductivity for aluminum is set as K_{Al} = 155W/m·K in the previous cases. For comparison, three cases with conductivity value equals 60, 200 and 400, by the unit of W/m·K are employed. From figure 25, the temperature and curvature versus time are shown.

From the comparison, the higher conductivity will endure less fluctuation of temperature. And the curvature change will be less significant. In actual experiment, if carbon steel is chosen as substrate, which has less conductivity, the stress of inside the specimen would be expected higher than that with aluminum substrate. Thus, it proves that YSZ tends to bond well to the aluminum substrate.

Furthermore, two cases are carried out to compare the effect of different specific heat of substrate. As shown in figure 26, different values of specific heat render different temperature the specimen obtain at steady state. Although lower specific heat, which indicates steel, takes less time to steady state, the temperature of the specimen is expected to be higher. Moreover, lower specific heat will make the specimen deform significantly, which may develop large stress during deposition process as well as cooling down process. Again, the result proves that aluminum is a better choice as substrate since it has higher conductivity and higher specific heat. This conclusion may not be very powerful since the lack of information of microstructure of bonds and the morphology of deposition particles, but in some sense, it proves the phenomenon by heat transfer view macroscopically.

6. Conclusion

In the present study, a valid nonlinear model of YSZ coating is employed in simulation. As discovered in experiments, the properties of coating represent as nonlinear elastic. To describe it, bimaterial model is introduced. Within the model, four variables are employed to represent the properties of coating. This model minimizes the number of variables as well as maintains the nonlinear stress-strain relationship. In order to obtain the properties through thermal cycle experiments, inverse analysis is adopted to extract stress-strain model by data of experiments. A Fortran program is used to generate data line in subroutine of Abaqus software to carry out the simulation.

After the preparation of material properties, a very detailed simulation is constructed according to actual thermal spray process of yttria stabilized zirconia (YSZ) coatings. The experiment is simplified from three-dimensional model into two-dimensional model. The factors in experiments are studied carefully, and a heat transfer model is used to describe the deposition process. Furthermore, in order to accomplish the deposition process, a program is used to generate new nodes and elements which represent the deposition particles which are added to existing model. The heat input is added though newly added nodes by concentrate method. The heat output is described by air convection though the free surface. After this, the simulation is carried out. With measurements of the temperature of the bottom of substrate and the curvature change of the specimen, same characteristics of experiments are captured in simulation. These include the oscillation generated by nozzle, the steady state of temperature measured and the increase of curvature.

Furthermore, to validate the simulation, several experiments are matched by investigate the temperature and curvature measurements. In these matching experiments, the simulation can obtain the same steady state temperature and the same value of curvature change. These results illustrate the validation of the simulation. Through these three cases, the value of heat input and output, the thickness of elements and the time of each single job is taken into attention. Some rules of these parameters are to be related to simulation results. After this, by the rule discovered, a case is predicted by simulation and the temperature value fit the experiments very well. Also, the parameter in experiments,

feed rate and raster speed are studied. Because the feed rate and raster speed in experiments are the dominating parameters of simulation such as heat input and output value, the element thickness and the single job time. Moreover, the simulations can help to record more than the experiments did. Three cases taken out in the previous section is employed to investigate the stress evolution through the TS deposition process. From the comparison, the higher feed rate renders higher residual stress. This is because higher feed rate brings in more heat and leads to larger temperature difference to form residual stress. In this same explanation, raster speed contributes opposite as feed rate does. Another scenario is with same deposition rate, the one with higher feed rate or lower raster speed would experience higher residual stress. Also, the stress evolution during the deposition process can be monitored. The stresses within the coating present a climbing trend during the process to approach the steady state. After reach the steady state, the stresses remain the same. The oscillation of stresses due to coating layers can be observed through deposition process either.

At last, the parameters within simulation are investigated to test the sensitivity of them. First, the effects of preheat temperature is studied. Simulations are starting from the different preheat temperatures, but the temperatures they reach at steady state is the same. Moreover, when investigating the curvature change, it is found that higher preheat temperature will lead lower increase of curvature during the deposition process. This means higher preheat temperature can cause less stress within the specimen. Then, by studying the heat transfer model, it is found that the higher value of heat input or the lower value of heat output would render higher increase of temperature value as well as the curvature value. But the curvature change is not that significant. Moreover, the properties of coating and substrate are studied. Lower modulus of coating renders smaller change of curvature during cooling down process. For substrate, higher conductivity will endure less fluctuation of temperature. And lower specific heat will make the specimen deform significantly, which may develop large stress during deposition process as well as cooling down process. The study of substrate properties reveals aluminum is a better choice as substrate since it has higher conductivity and higher specific heat.

In a word, this simulation help to study TS process in quantities level and obtain better visible results. It would be a very powerful auxiliary tool in TS industry.

References

Basu, D., Funke, C. and Steinbrech, R.W. 1999. Effect of Heat Treatment on Elastic Properties of Separated Thermal Barrier Coatings. J. Mater. Res., 14(12), pp. 4643-50.

Carlotti, G., Doucet, L., Dupeux, M., 1997. Elastic properties of silicon dioxide films deposited by chemical vapour deposition from tetraethylorthosilicate. Thin Solid Films 296, 102–105.

Eldridge, J.I., Morscher, G.N. and Choi, S.R. 2002. Quasistatic vs. Dynamic Modulus Measurements of Plasma Sprayed Thermal Barrier Coatings. Ceram. Eng. Sci. Proc., 23, pp. 371-80.

Harok, V., Neufuss, K., 2001. Elastic and inelastic effects in compression in plasma-sprayed ceramic coatings. Journal of Thermal Spray Technology 10 (1), 126–132.

Hunsche, B., Vergo¨ hl, M., Neuha¨user, H., Klose, F., Szyszka, B., Matthe´e, T., 2001. Effect of deposition parameters on optical and mechanical properties of MF- and DC-sputtered Nb2O5 films. Thin Solid Films 392 (2), 184–190.

Kesler, O., Matejicek, J., Sampath, S., Suresh, S., Gnaeupel-Herold, T., Brand, P.C., Prask, H.J., 1998. Measurement of residual stress in plasma-sprayed metallic, ceramic and composite coatings. Materials Science and Engineering A 257, 215–224.

Kim, S.R. and Nairn, J.A. 2000. Eng. Frac. Mech. **65,** 573.

Kroupa, F., Dubsky, J., 1999. Pressure dependence of Young's moduli of thermal sprayed materials. Scripta Materialia 40 (11), 1249–1254.

Kroupa, F., Plesek, J., 2001. Bending of beams with elastically non-liner coatings. Journal of Thermal Spray Technology Volume 11(4), 508 – 516.

Kroupa, F., Plesek, J., 2002. Nonlinear elastic behavior in compression of thermally sprayed materials. Materials Science and Engineering A 328, 1–7.

Krulevitch, P., Ramsey, P.B., Makowiecki, D.M., Lee, A.P., Northrup, M.A., Johnson, G.C., 1996. Mixed-sputter deposition of Ni–Ti–Cu shape memory films. Thin Solid Films 274, 101–105.

Kucuk, A., Berndt, C.C., Senturk, U., Lima, R.S. and Lima, C.R.C. 2000 Influence of Plasma Spray Parameters on Mechanical Properties of Yttria Stabilized Zirconia Coatings: Four Point Bending Test. Mater. Sci. Eng. A.,284, pp. 29-40.

Kuroda, S., Fukushima, T., Kitahara, S., 1988. Simultaneous measurement of coating thickness and deposition stress during thermal spraying. Thin Solid Films 164, 157–163.

Kuroda, S., Fukushima, T., Kitahara, S., 1990. Generation mechanisms of residual stresses in plasma-sprayed coatings. Vacuum 41, 1297–1299.

Lacquaniti, V., Monticone, E., Picotto, G.B., 1997. Structural and surface properties of sputtered Nb films for multilayer devices. Surface Science 377–379, 1042–1045.

Liu. Y, et al., Non-linear elastic properties of plasma-sprayed zirconia coatings and associated relationships with processing conditions, Acta Mater (2007), doi:10.1016/ j.actamat. 2007. 04.037

Liu. Y, et al., Anelastic Behavior of Plasma-Sprayed Zirconia Coatings, J. Am. Ceram. Soc., 91 [12] 4036–4043 (2008) DOI: 10.1111/j.1551-2916.2008.02789.x

Matejicek, J., Sampath, S., Gilmore, D., Neiser, R., 2003. In situ measurement of residual stresses and elastic moduli in thermal sprayed coatings: Part 2: processing effects on properties of Mo coatings. Acta Materialia 51, 873–885.

Menzel, S., Strehle, S., Wendrock, H., Wetzig, K., 2005. Effect of Ag-alloying addition on the stress–temperature behavior of electroplated copper thin films. Applied Surface Science 252, 211–214.

Nakamura, T., Liu, Y. 2006. Determination of nonlinear properties of thermal sprayed ceramic coatings via inverse analysis. International Journal of Solids and Structures 44 (2007) 1990–2009.

Nohava, J., Kroupa. F. 2005. Nonlinear stress-strain behavior of plasma sprayed ceramic coatings. Acta technica ČSAV, vol. 50, n°3, pp. 251-262

Oka, Y., Tao, M., Nishimura, Y., Azuma, K., Fujiwara, E., Yatsuzuka, M., 2003. Properties of thick DLC films prepared by plasmabased ion implantation and deposition using combined RF and H.V. pulses. Nuclear Instruments and Methods in Physics Research B 206, 700–703.

Steinbrech, R.W. 2002. Thermomechanical Behavior of Plasma Sprayed Thermal Barrier Coatings. Ceram. Eng. Sci. Proc., 23, pp. 379- 408.

Stoney, G., 1909. The tension of metallic films deposited by electrolysis. Proc Roy Soc London A 82, 172–175.

Tsui, Y.C., Clyne, T.W., 1997. An analytical model for predicting residual stresses in progressively deposited coatings: Part 1: planar geometry. Thin Solid Films 306, 23–33.

Waki, H., Ogura, K., Nishikawa, I., Ohmori, A., 2004. Monotonic and cyclic deformation behavior of plasma-sprayed coatings under uniaxial compressive loading. Materials Science and Engineering A 374, 129–136.

Wang, W., Li, C., Wang, Y., Yang, G., Sonoya, K., 2006. Tensile deformation behavior of plasma-sprayed Ni–45Cr coatings. Surface and Coatings Technology 201, 842–847.

Appendix

Summary of program to generates nodes and elements. It can write abaqus input file and then submit to server, read the temperature and curvature information throughout the simulation

```
Setup the variables;
      Define Element Thickness;
      Set numbers of passage;
      Set the place of sensor to record displacement and temperature;
      Define the interval to save files
End Setup

Loop by number of passages

      Loop by number of elements for single layer

            Do read data from result
                  Define file to copy temperature information;
                  Define file to copy curvature information;
                  Read temperature;
                  Calculate curvature;
            End read files

            Do generate new nodes
                  Generate new node by constant change in x-axis and
                  setup of element thickness in y-axis;
                  Write new nodes number in certain file;
            End add new nodes

            Do generate new elements
                  Generate new elements by newly added nodes;
                  Write new elements number in certain file;
            End add new elements

            Delete unnecessary files

            Do write Abaqus input file
                  Restart from predessor job;
                  Input geometric model;
                  Include nodes files, set top of them as heat input
                  position;
                  Include elements files;
                  Define material propeties of coating and substrate;
                  Define heat transfer model;
                  Record temperature and displacement;
                  Record stress evolution;
            End write Abaqus input file

            Submit to simulate
      End loop
End loop
```

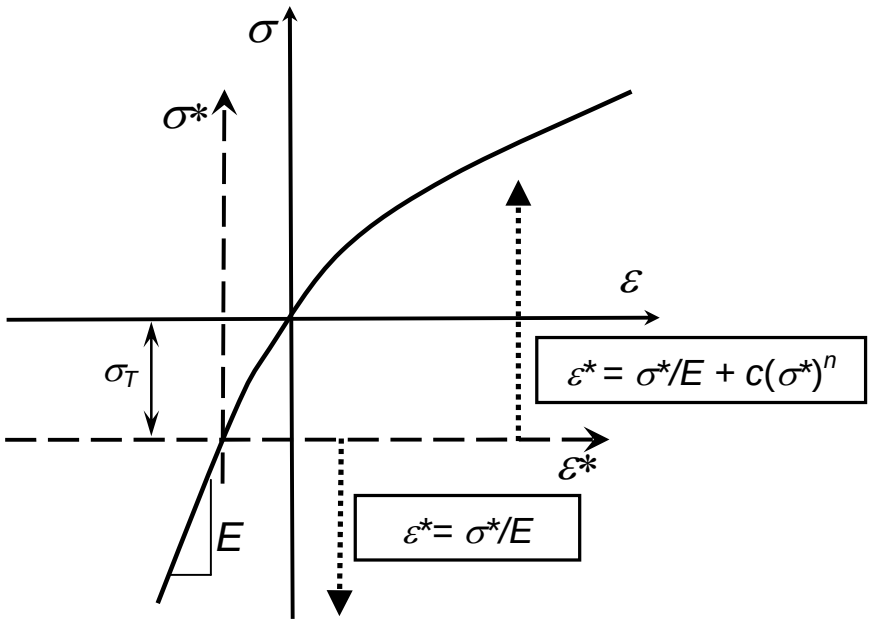

Figure 1. Nonlinear stress-strain relation model for TS ceramic coatings. Change in linear and nonlinear stress-strain relation occurs at transitional stress σ_T. Corresponding equations are noted below and above the ε^* axis, respectively.

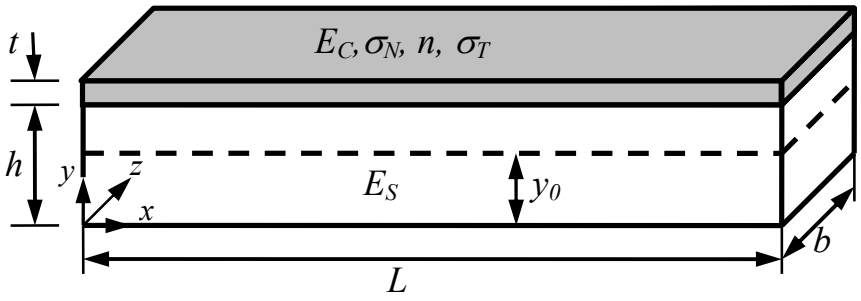

Figure 2. Schematic of TS coating on substrate with relevant dimensions. Corresponding material parameters are noted and the location of neutral axis y_o is shown.

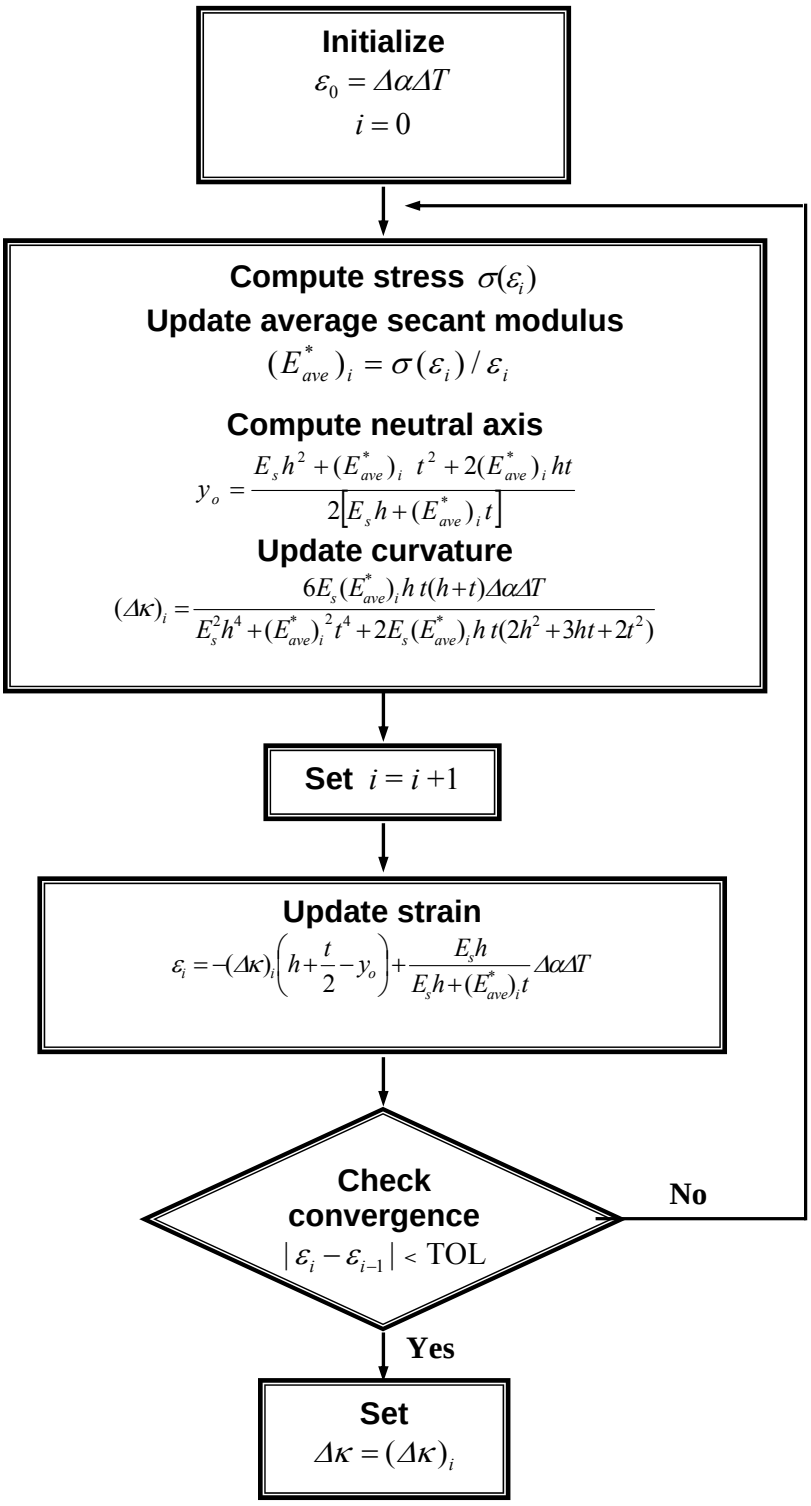

Figure 3. Flowchart to compute curvature change $\Delta\kappa$ for a given moment change ΔT.

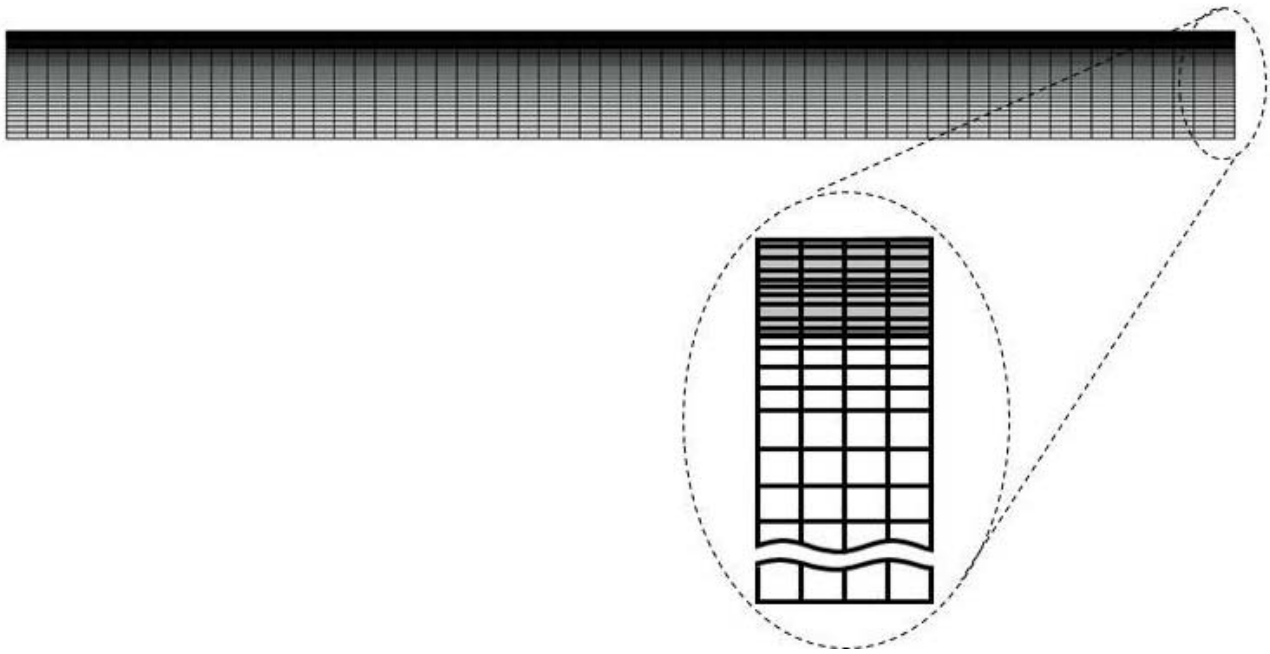

Figure 4. Finite element model of YSZ coating beam. 26700 elements are used in the model. Smaller elements are required for coatings to simulate the nonlinear properties and avoid inconsistent results in stress and strain.

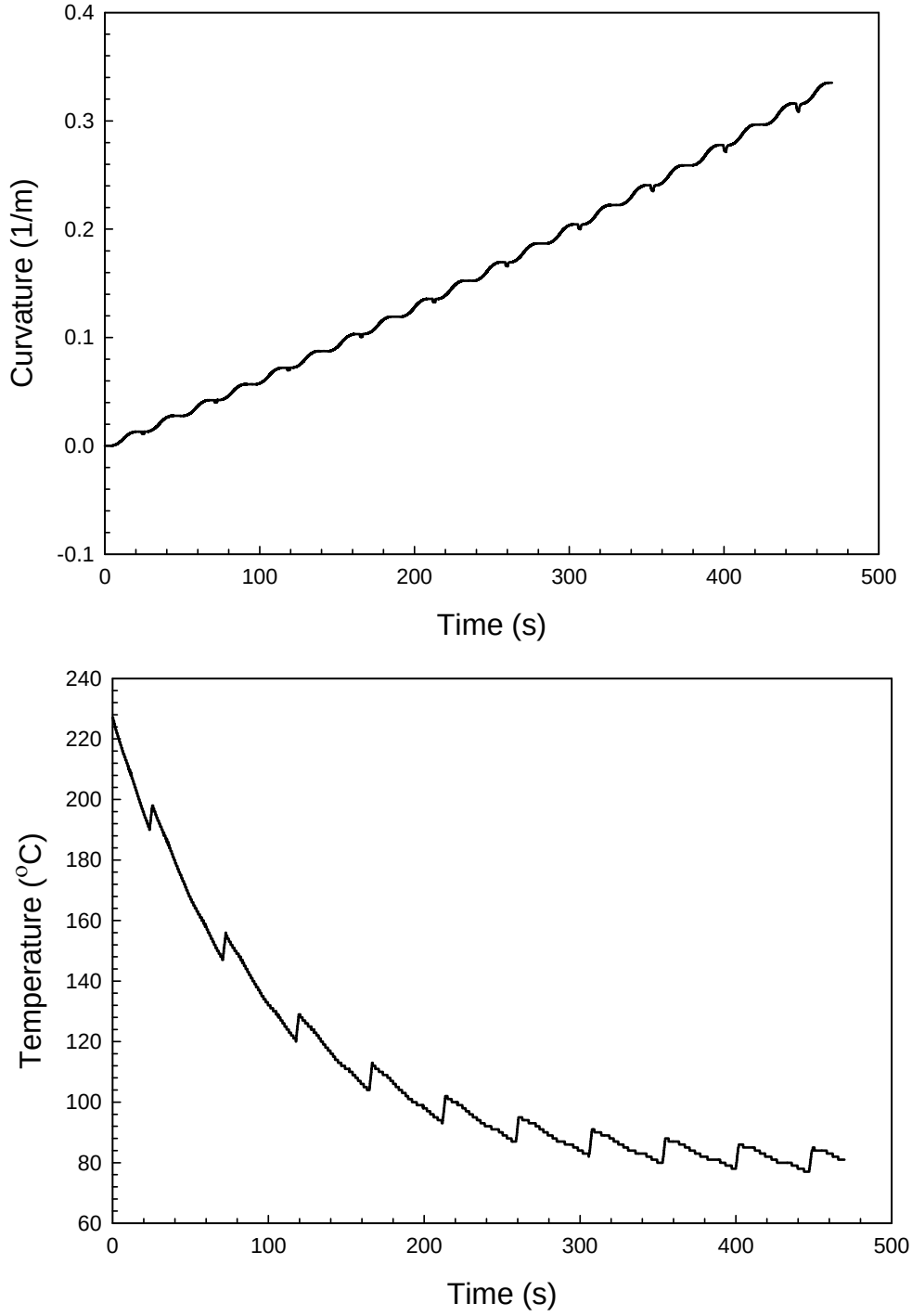

Figure 5. Simulated curvature and temperature results from simulation with high deposition temperature but no heat energy input.

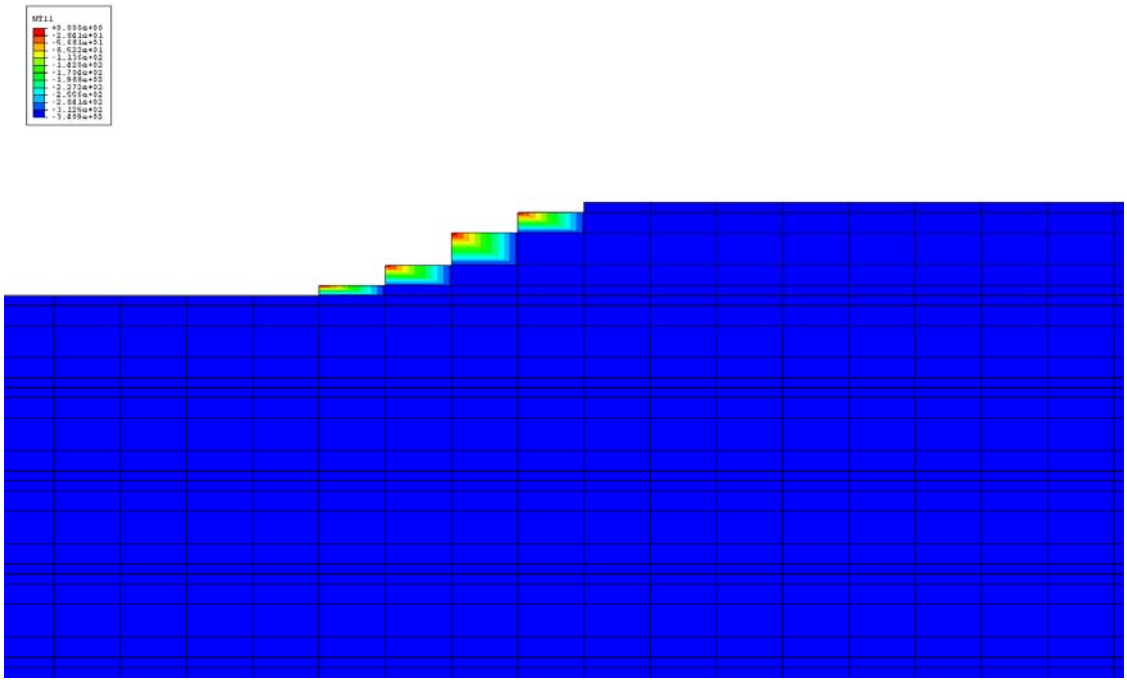

Figure 6. Temperature field distribution of new added nodes in certain deposition job.

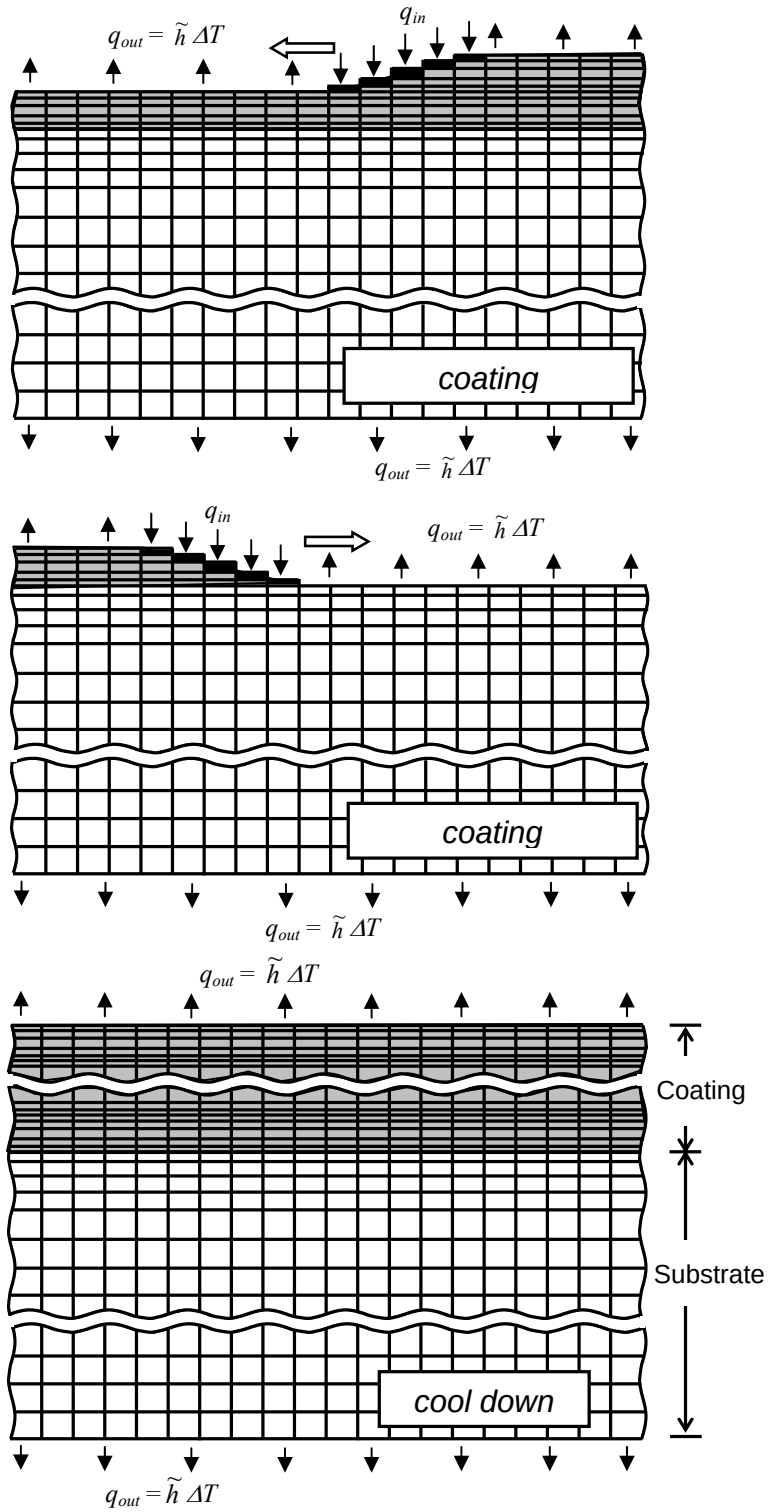

Figure 7. Accurate simulation of thermal spray deposition process through adding elements along transverse direction under proper heat transfer. The bottom figure shows cool down of completed deposition.

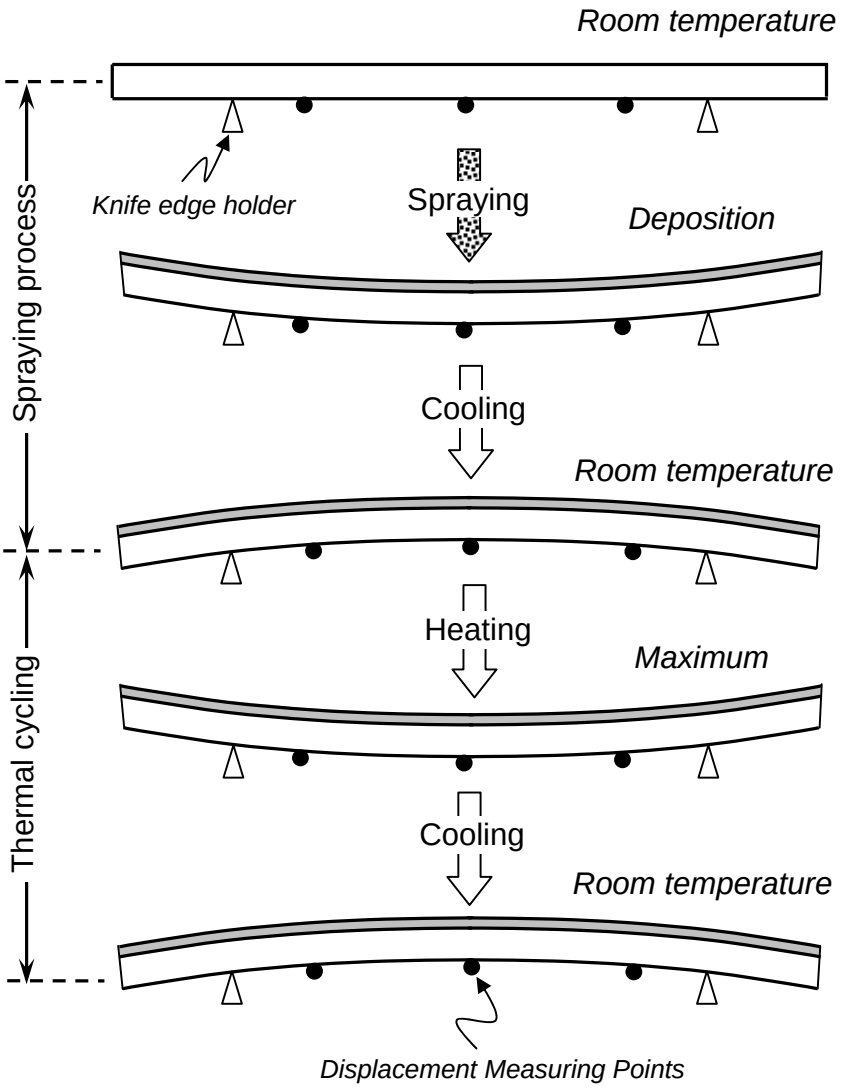

Figure 8. Schematic of curvature change as coating and substrate is thermally sprayed and thermal cycled. ICP sensor in placed at the bottom of substrate. Three points of measurements report the curvature change throughout the deposition process and cooling down process.

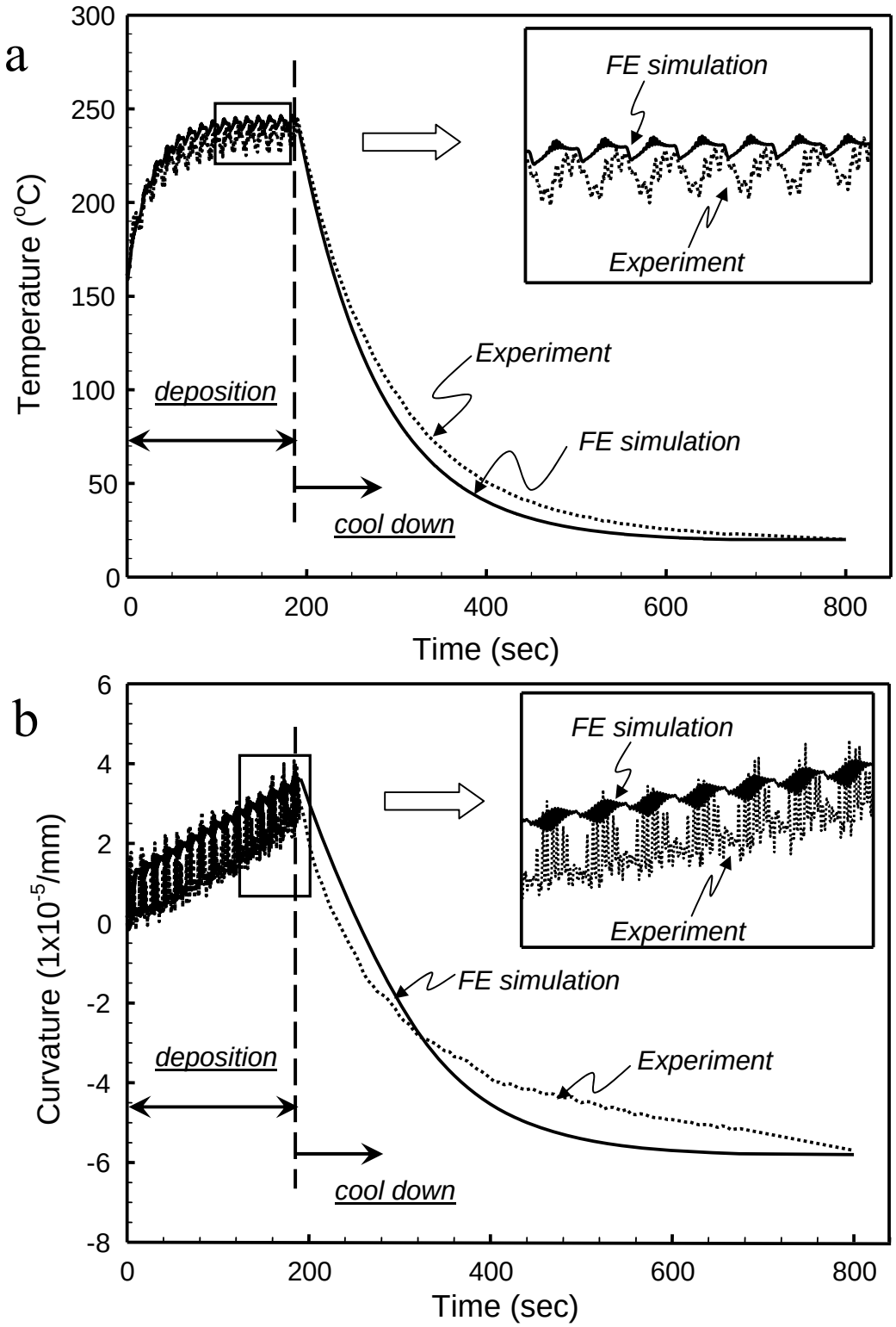

Figure 9. Simulated (a) temperature and (b) curvature results from simulation. For comparison experimental results are also shown. Magnified curves in insets have different coordinate scales.

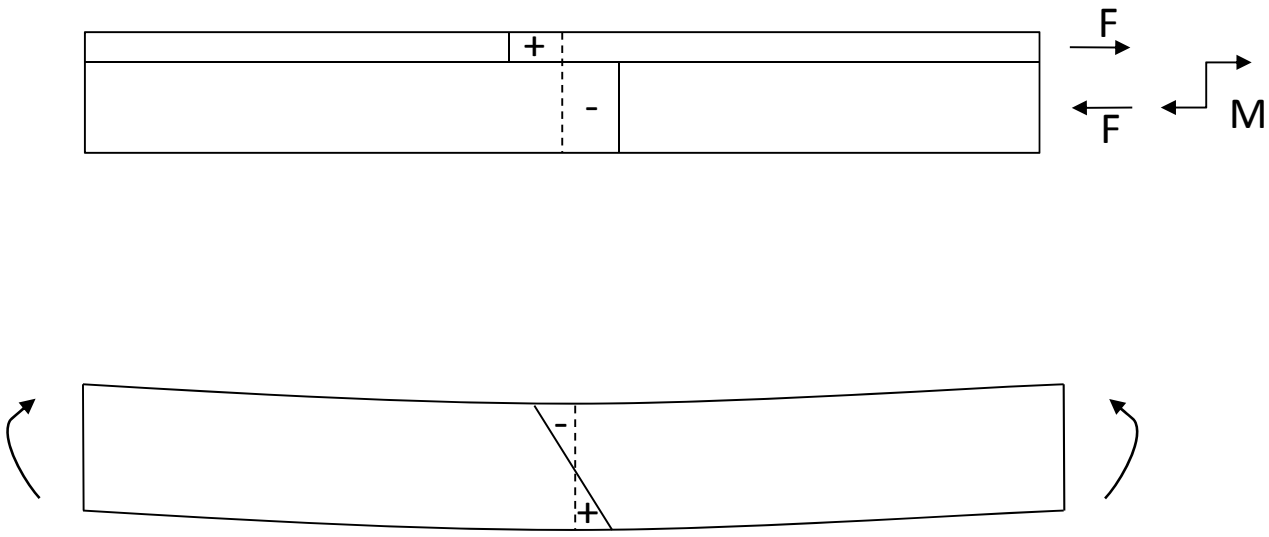

Figure 10. Schematic figure of stress within the specimen. The tension is defined as positive value. The compression is defined as minus value. The deform is derived from the bending caused by different CTE (coefficient thermal expansion) during deposition process.

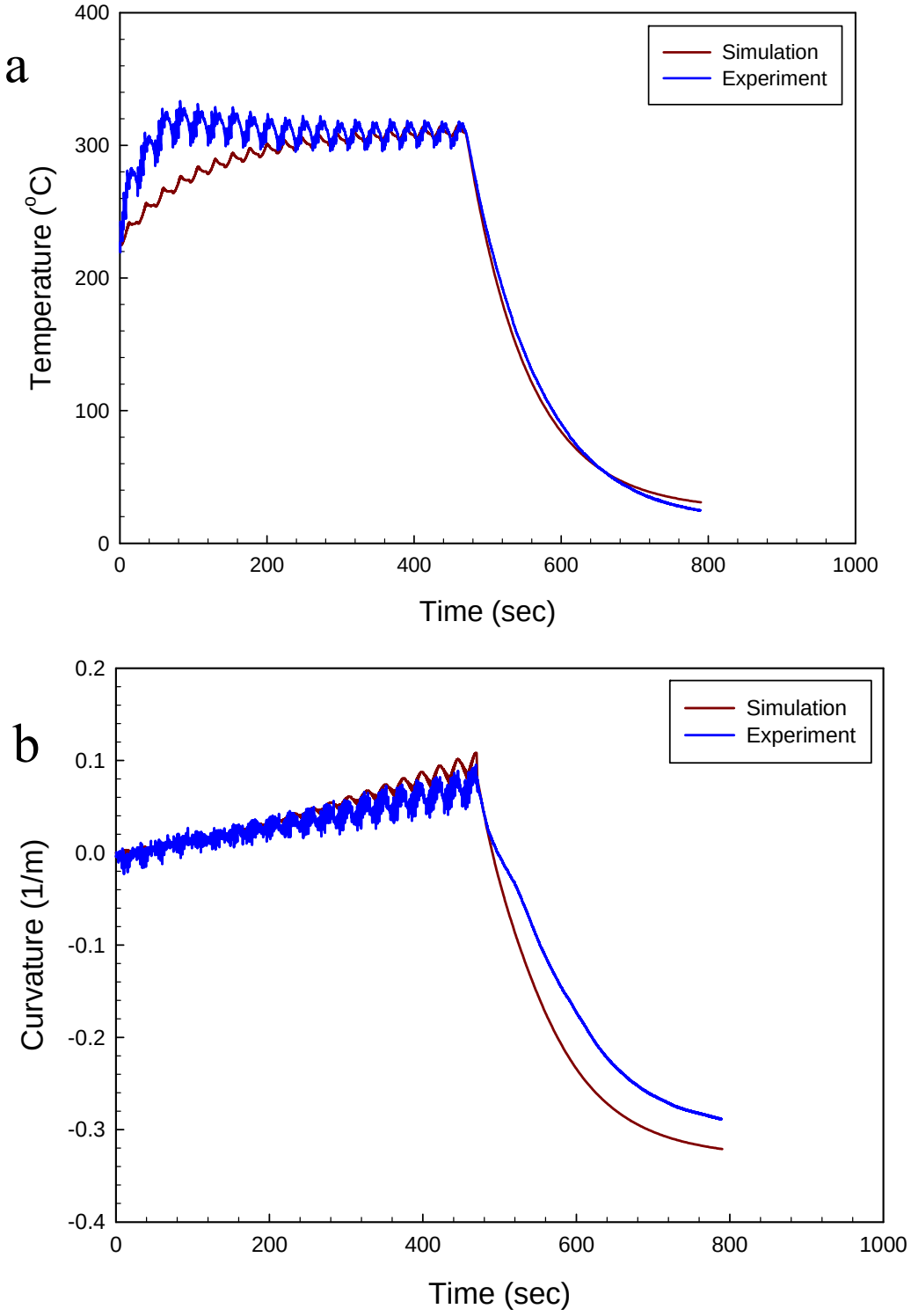

Figure 11. Comparison between experiment and simulation of (a) temperature and (b) curvature results of experiment R918. The red line stands for the simulation results. As (a) shows, the simulation takes longer time to reach the steady state. While the value of temperature fits well. In (b), the curvature of simulation has less oscillation.

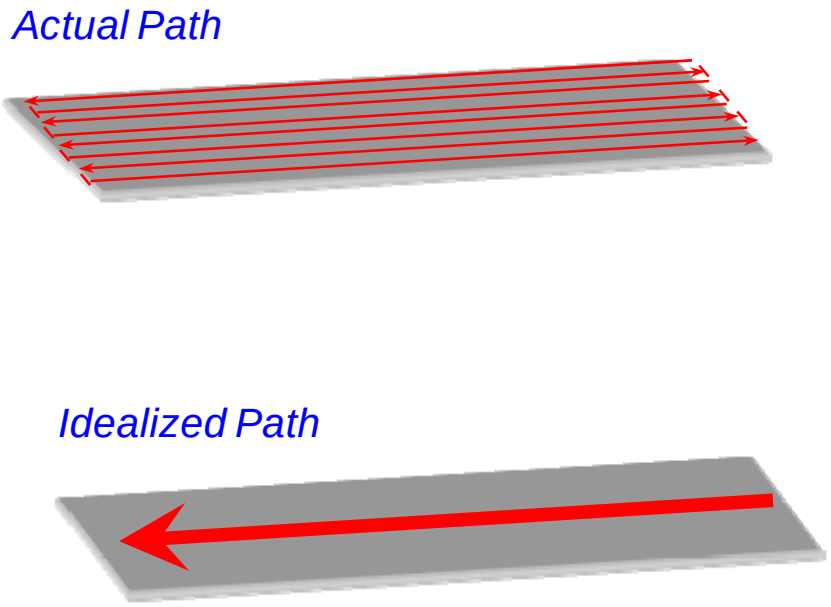

Figure 12. Raster path in TS deposition process vs. simulation. The simulation adopts two dimensional model, which cannot present lattice path style in experiments.

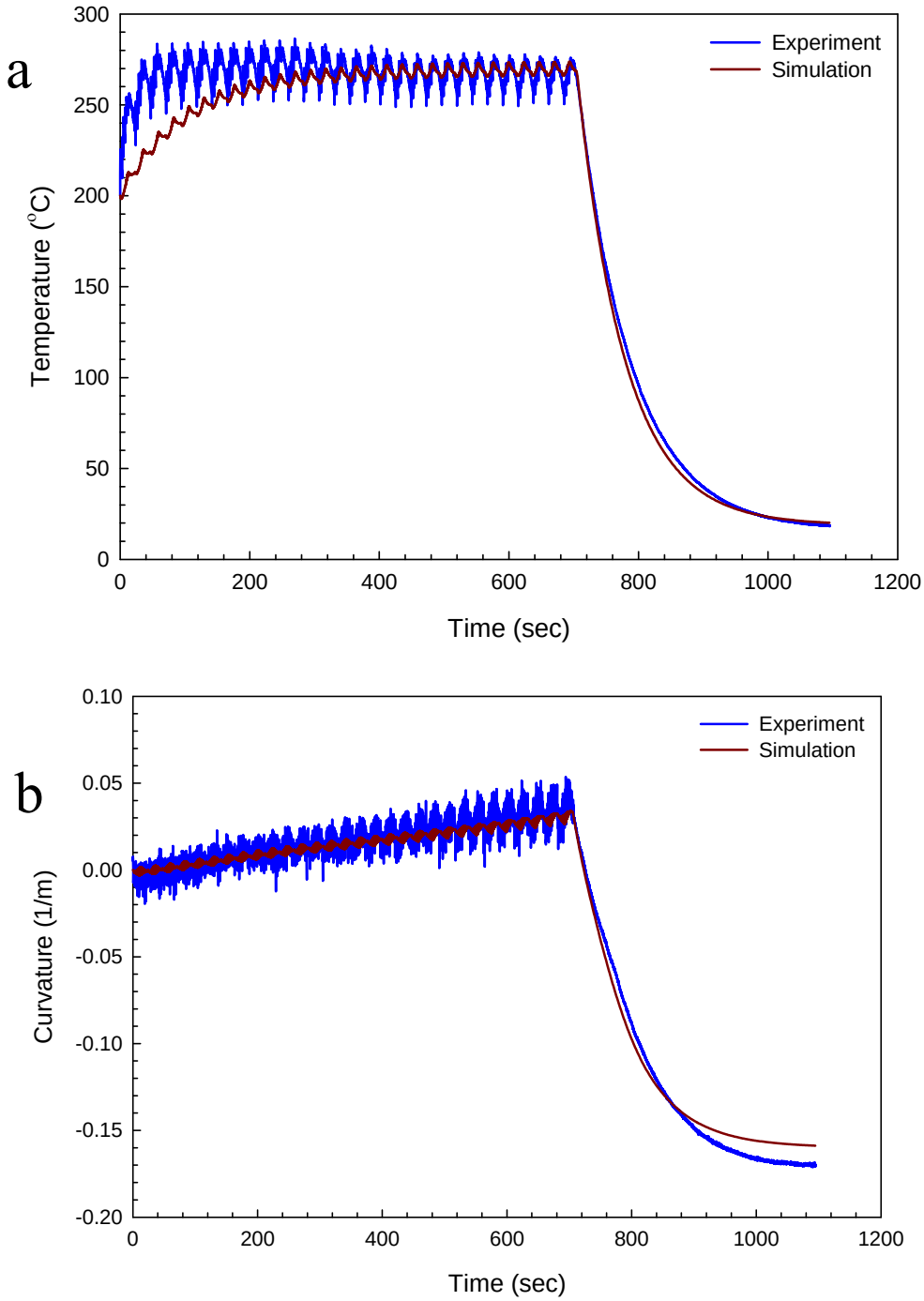

Figure 13. Comparison between experiment and simulation of (a) temperature and (b) curvature results of experiment R920. Better match results due longer deposition time.

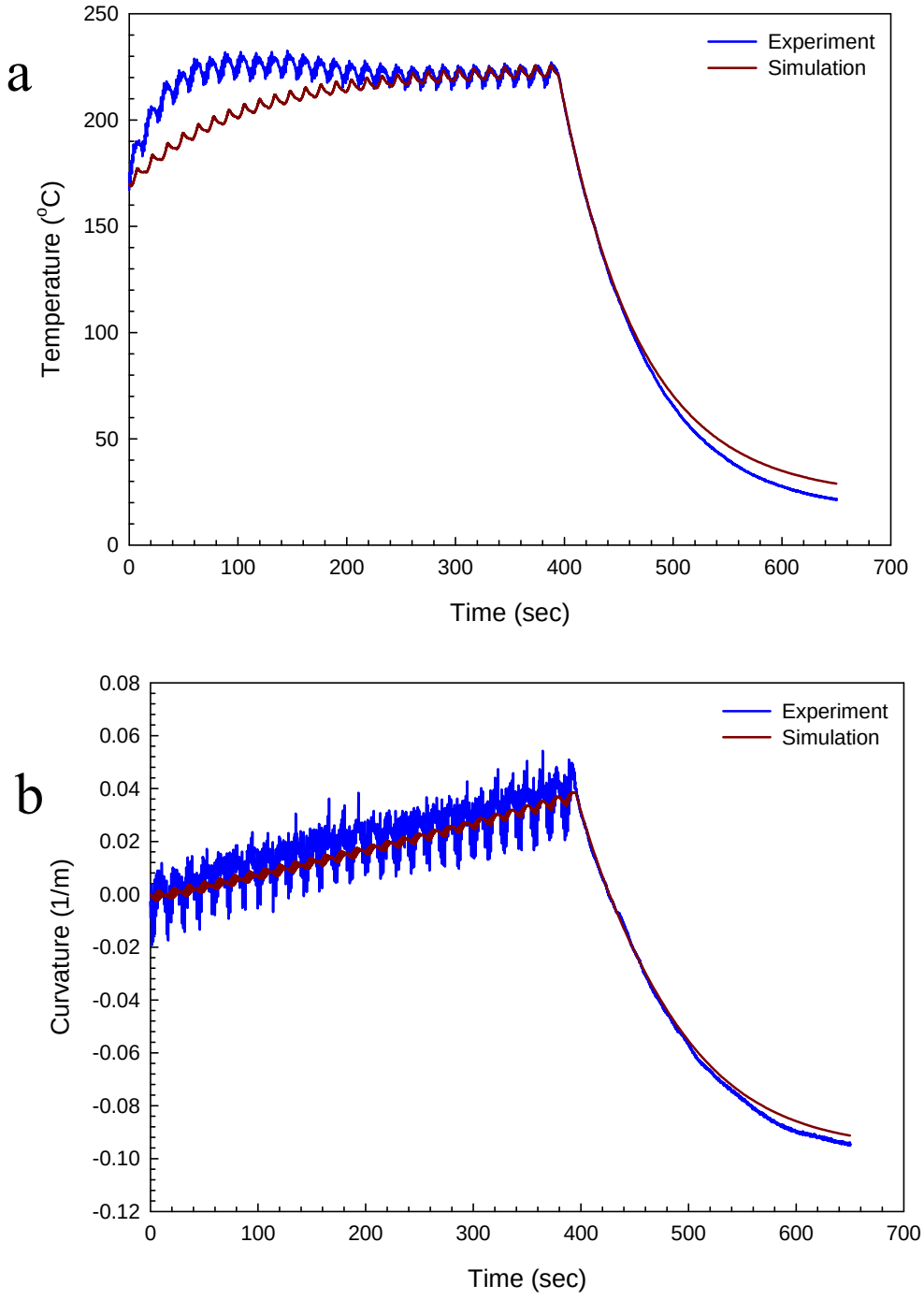

Figure 14. Comparison between experiment and simulation of (a) temperature and (b) curvature results of experiment R922. Due to small difference of steady state temperature and preheat temperature, the simulation reach the steady state quickly.

Figure 15. Raster path of experiment. The lattice paths are raster path of nozzle. The red rectangle is sample, fixed by four dots. There are extra path of raster other than on the specimen.

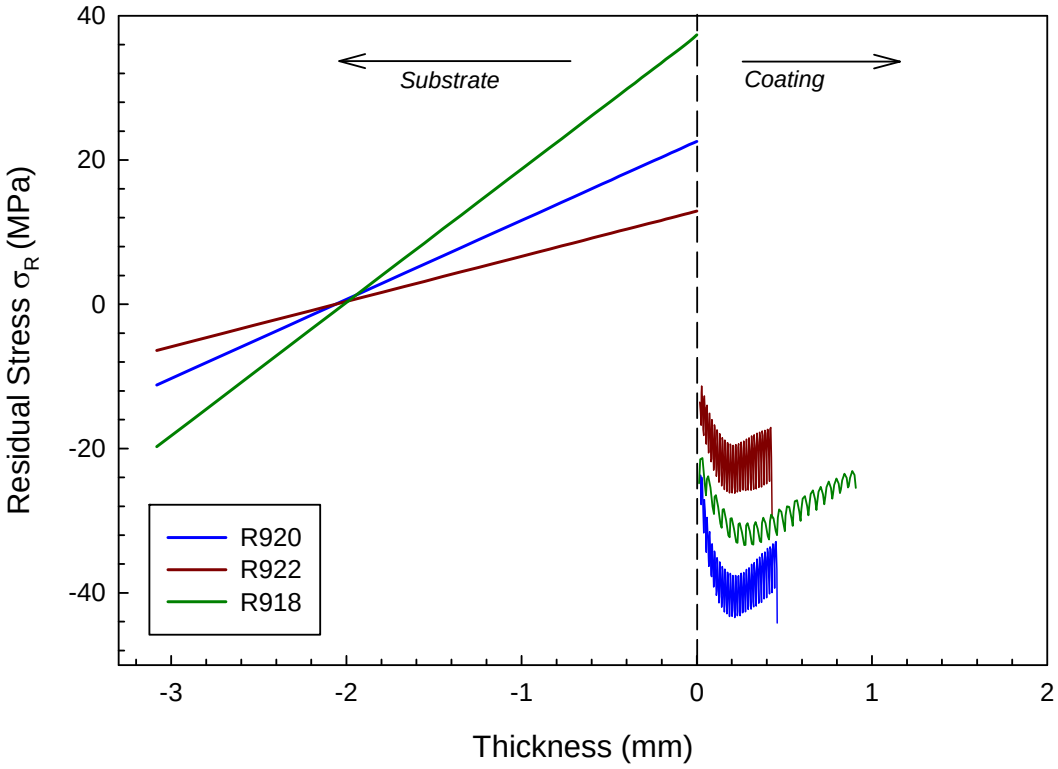

Figure 16. Residual stress through thickness of specimens. Left side of the dash line are substrates, the right side are coatings. Zero marks the interface.

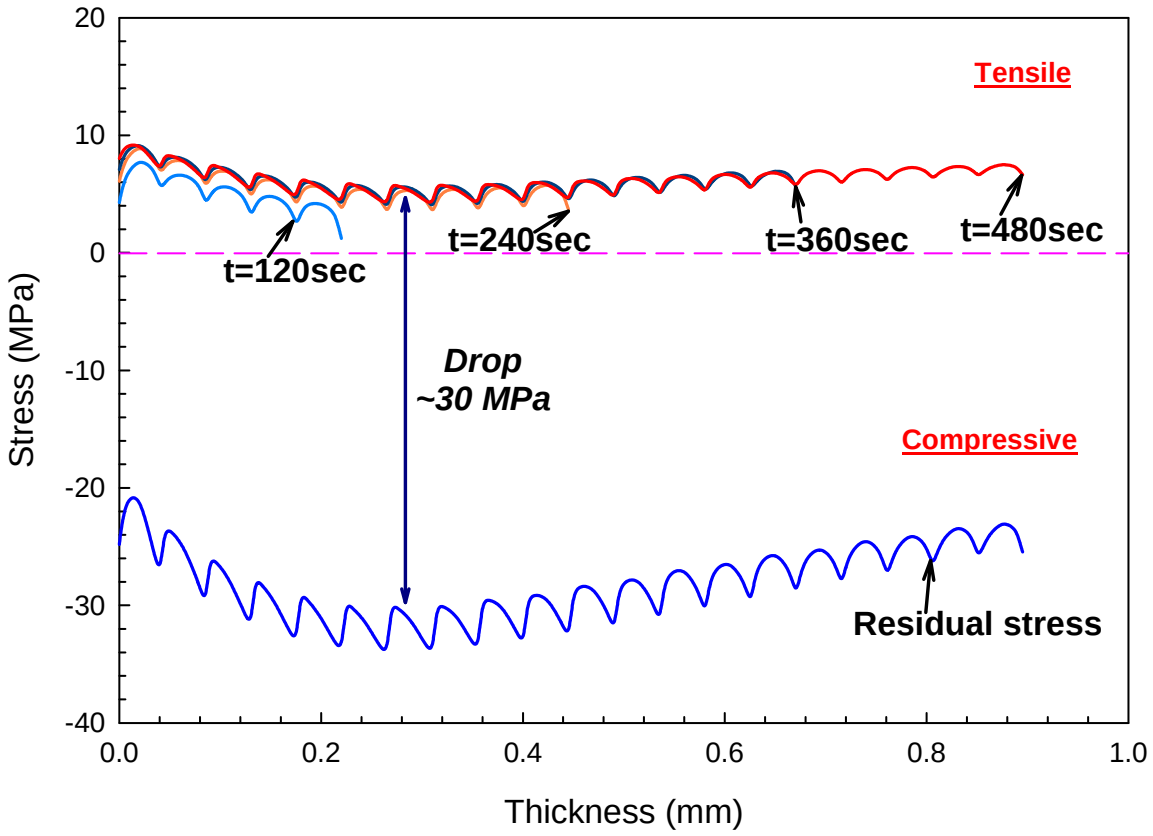

Figure 17. Stress evolution during the deposition process and residual stress after cooling down within YSZ coating of R918. Zero of x axis means the interface with substrate. Four moment of deposition process (120 sec, 240 sec 360 sec and 480 sec) are recorded. The dash line remarks the interface of tensile stress and compressive stress.

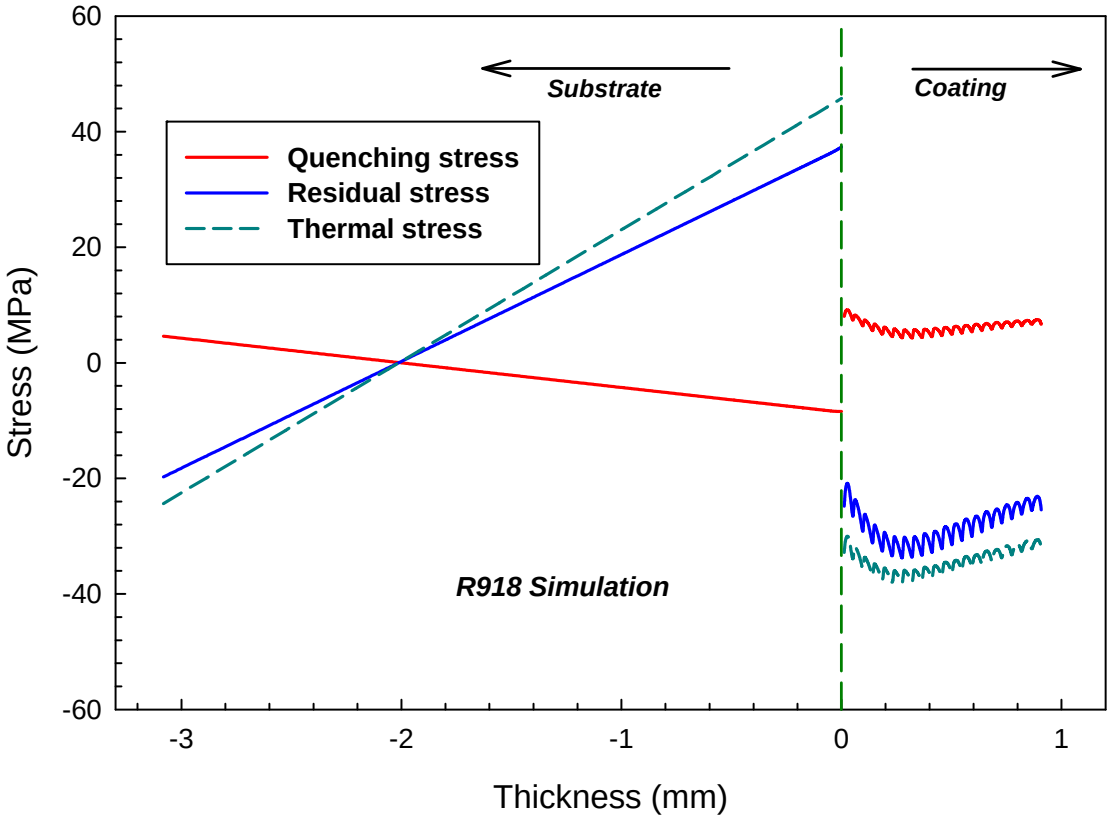

Figure 18. Quenching stress and residual stress within specimen of R918. Zero of x axis means the interface of coating and substrate. The left side is substrate, the right side is coating.

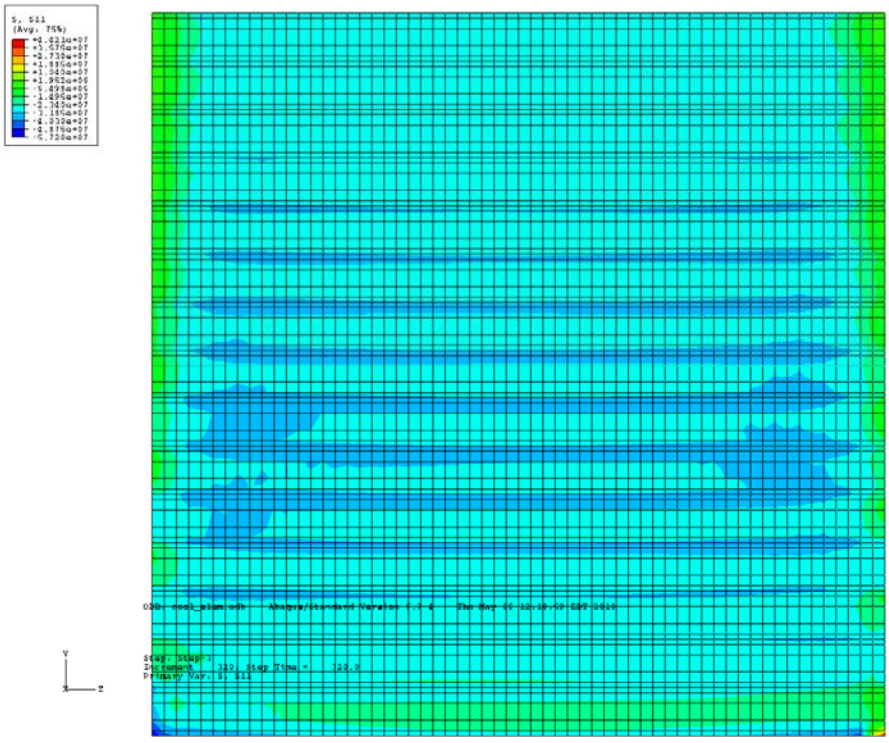

Figure 19. Coating residual stress profile of R918 after cooling down.

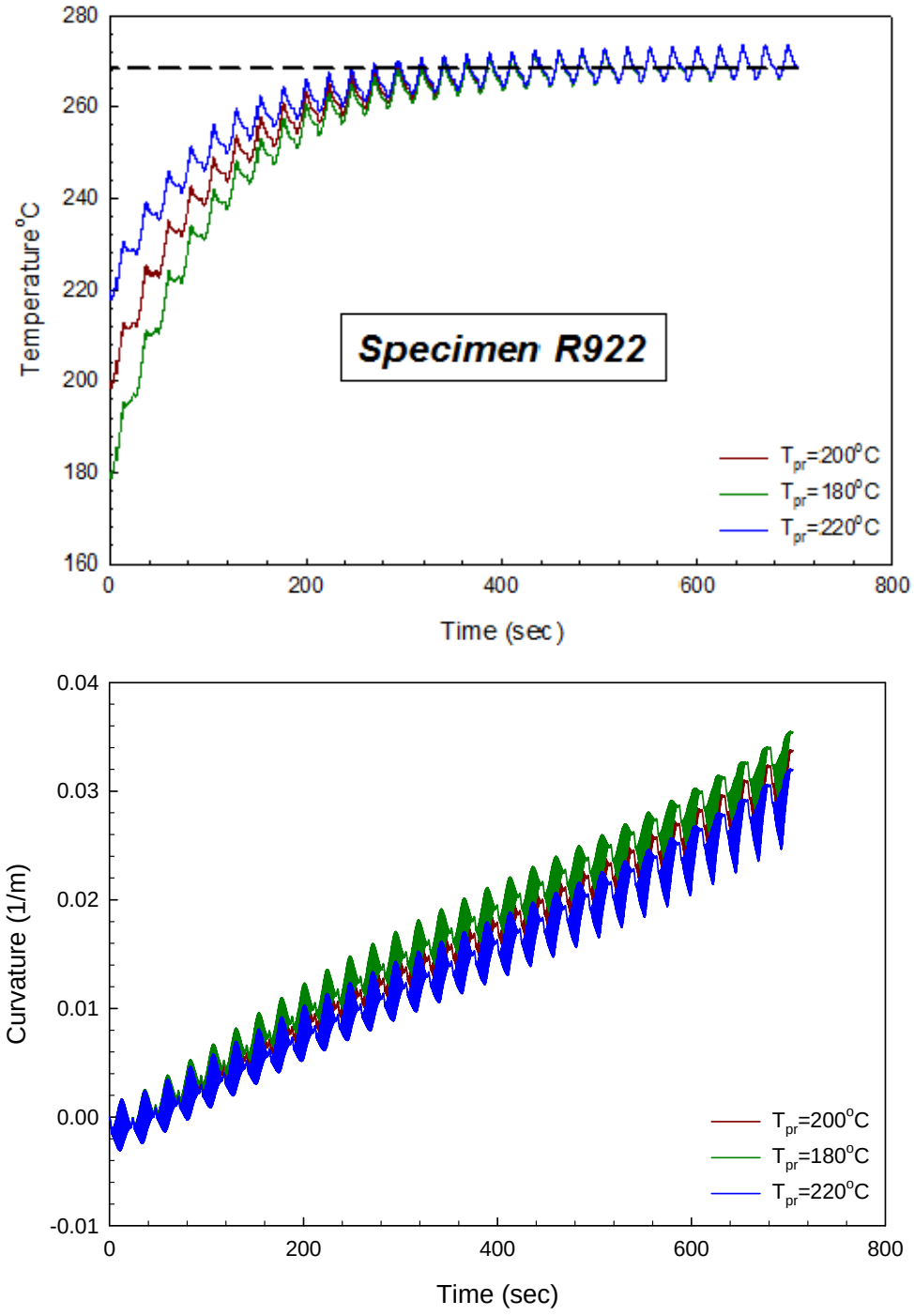

Figure 20. Different preheat temperature simulation comparing the simulation of specimen R920.

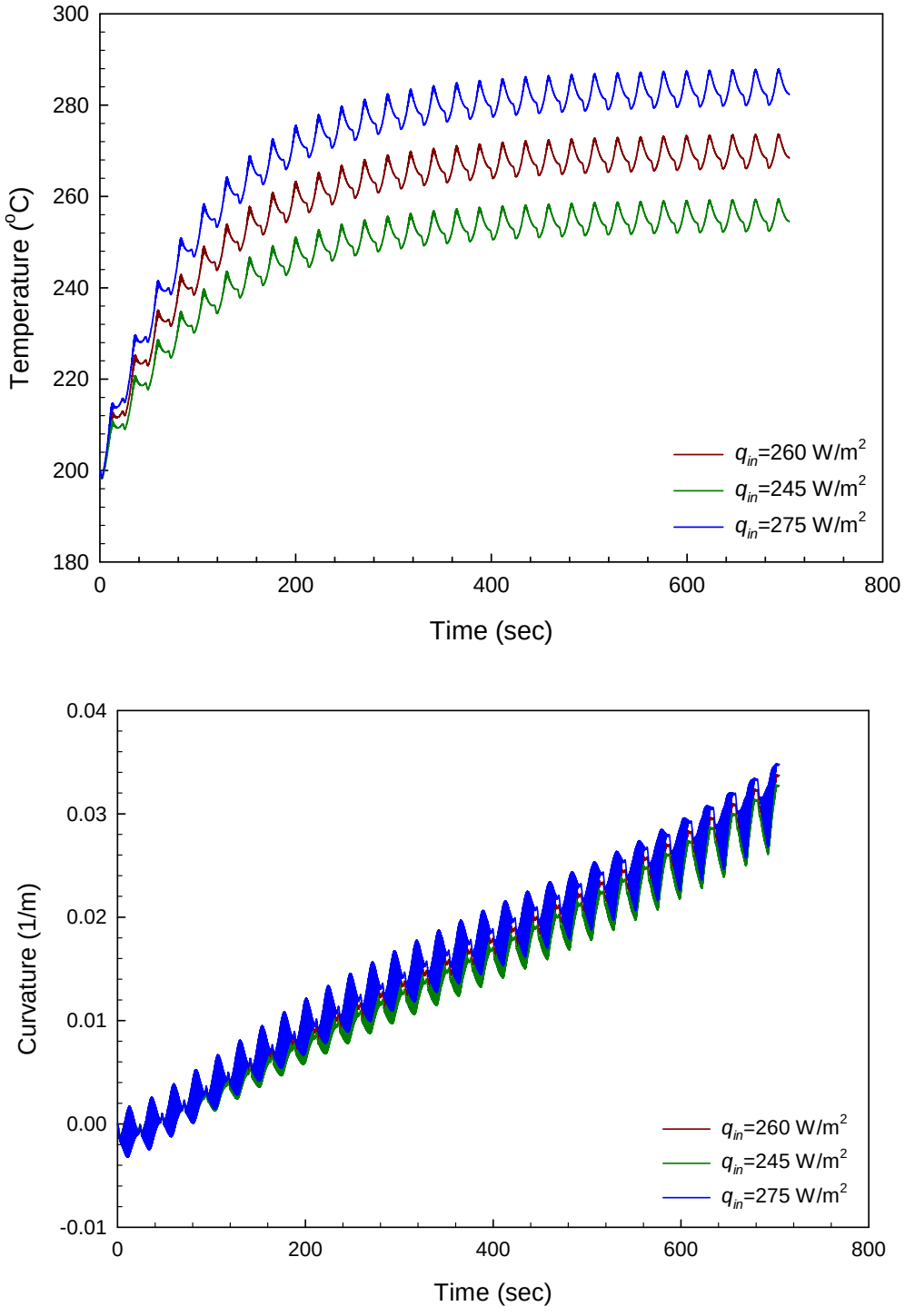

Figure 21. Different heat input values of simulations comparing the simulation of specimen R920.

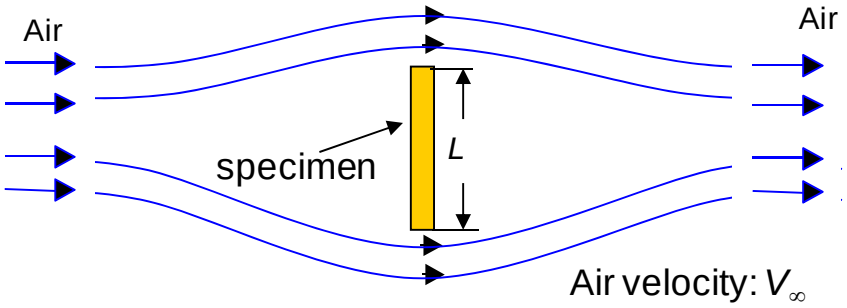

Figure 22. Schematic model of convection condition in deposition process as well as cooling down process.

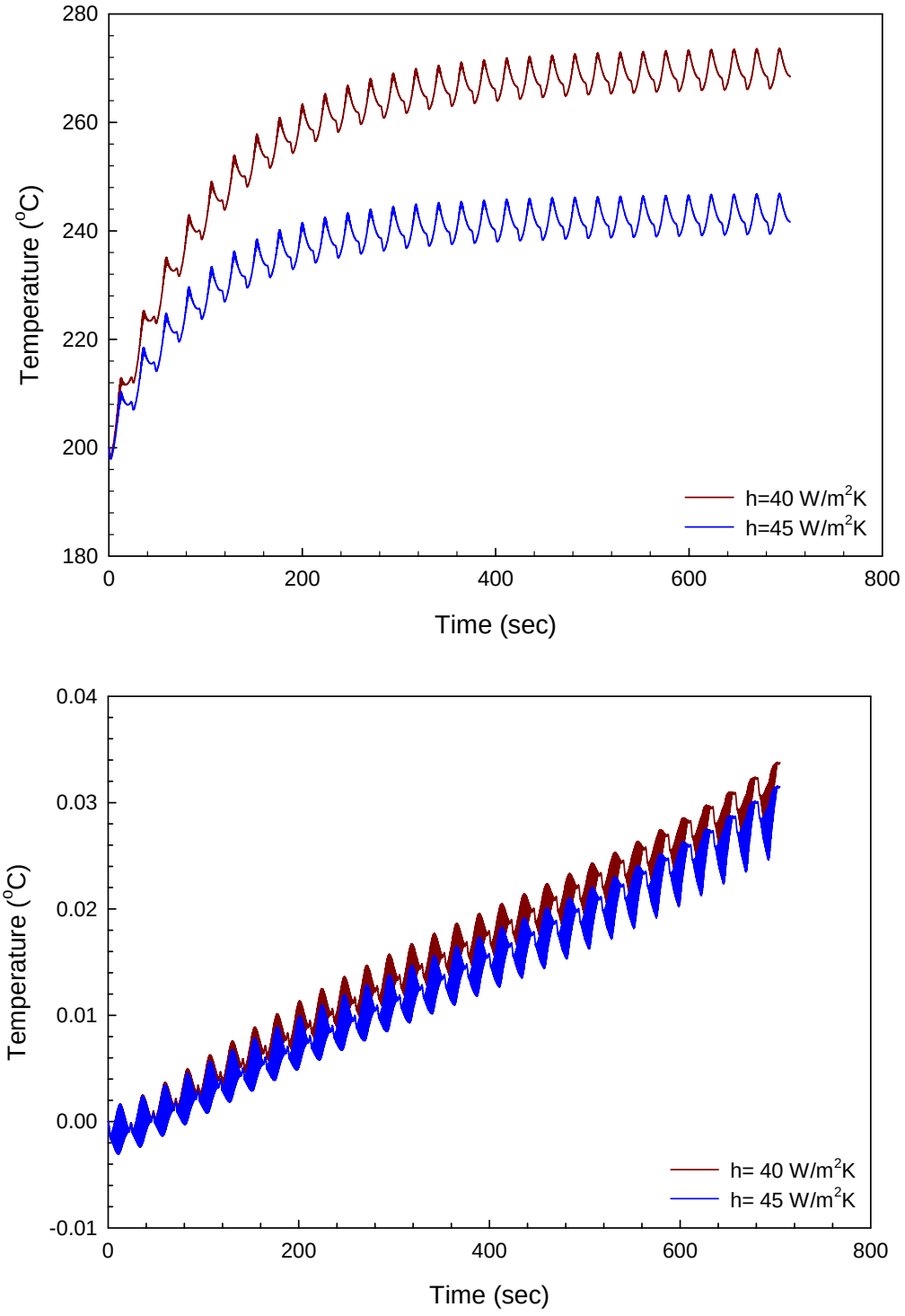

Figure 23. Different heat output values of simulations comparing the simulation of specimen.

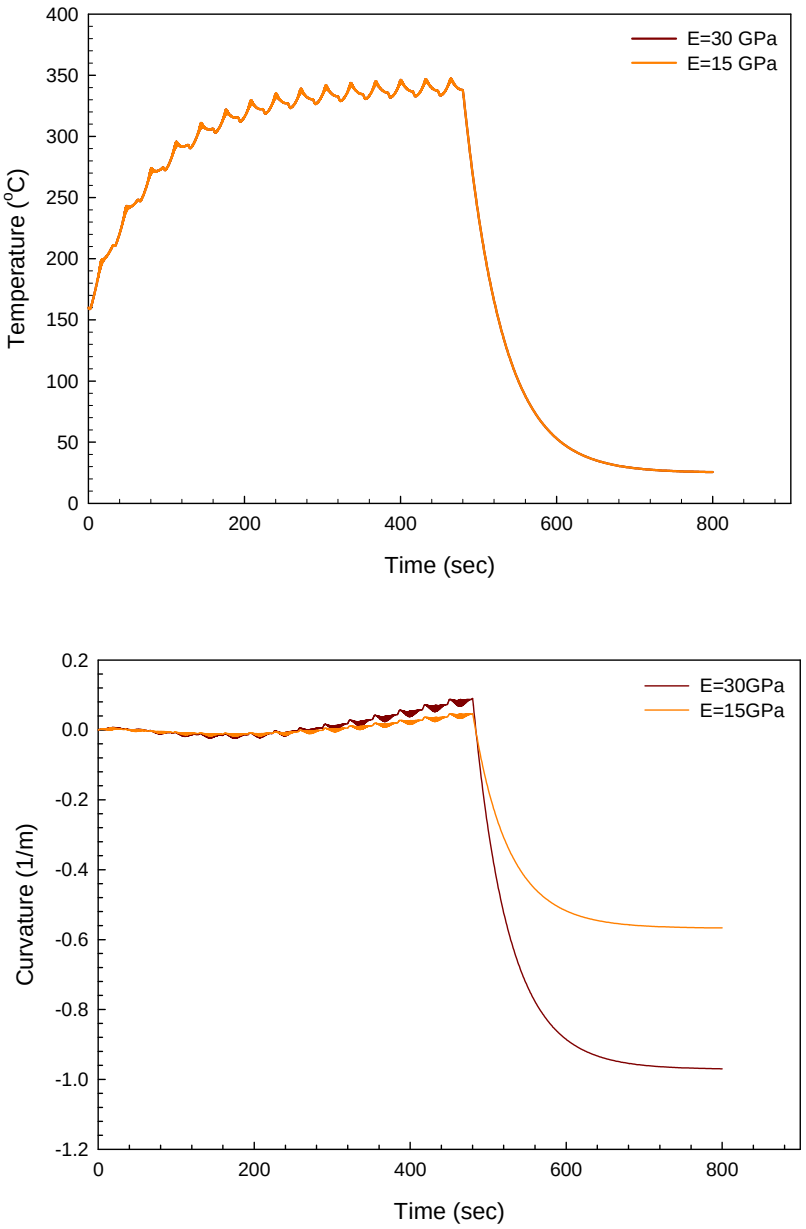

Figure 24. Trial simulation with different value of linear properties in coating.

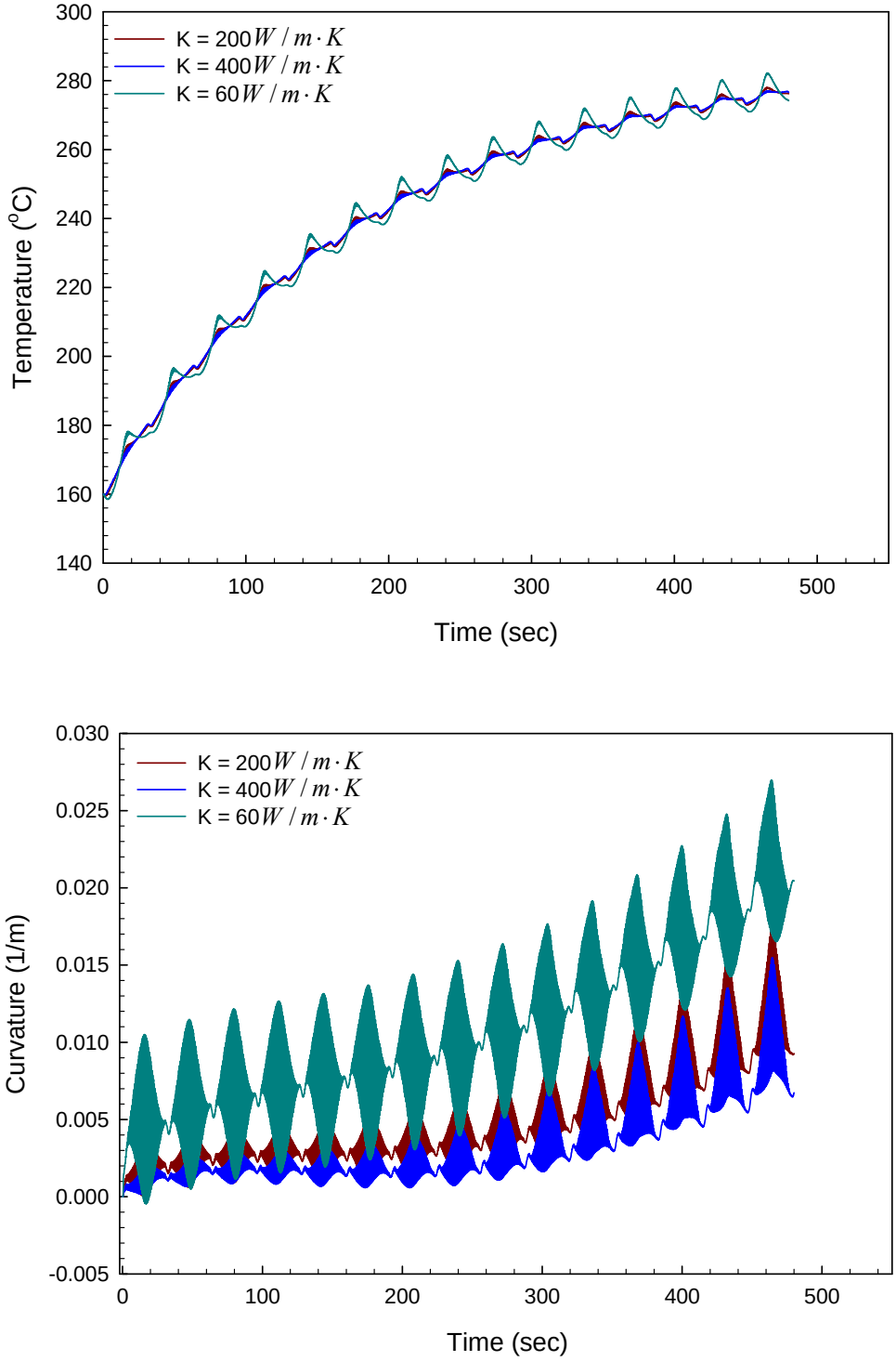

Figure 25. Deposition simulation with different value of conductivity of substrate.

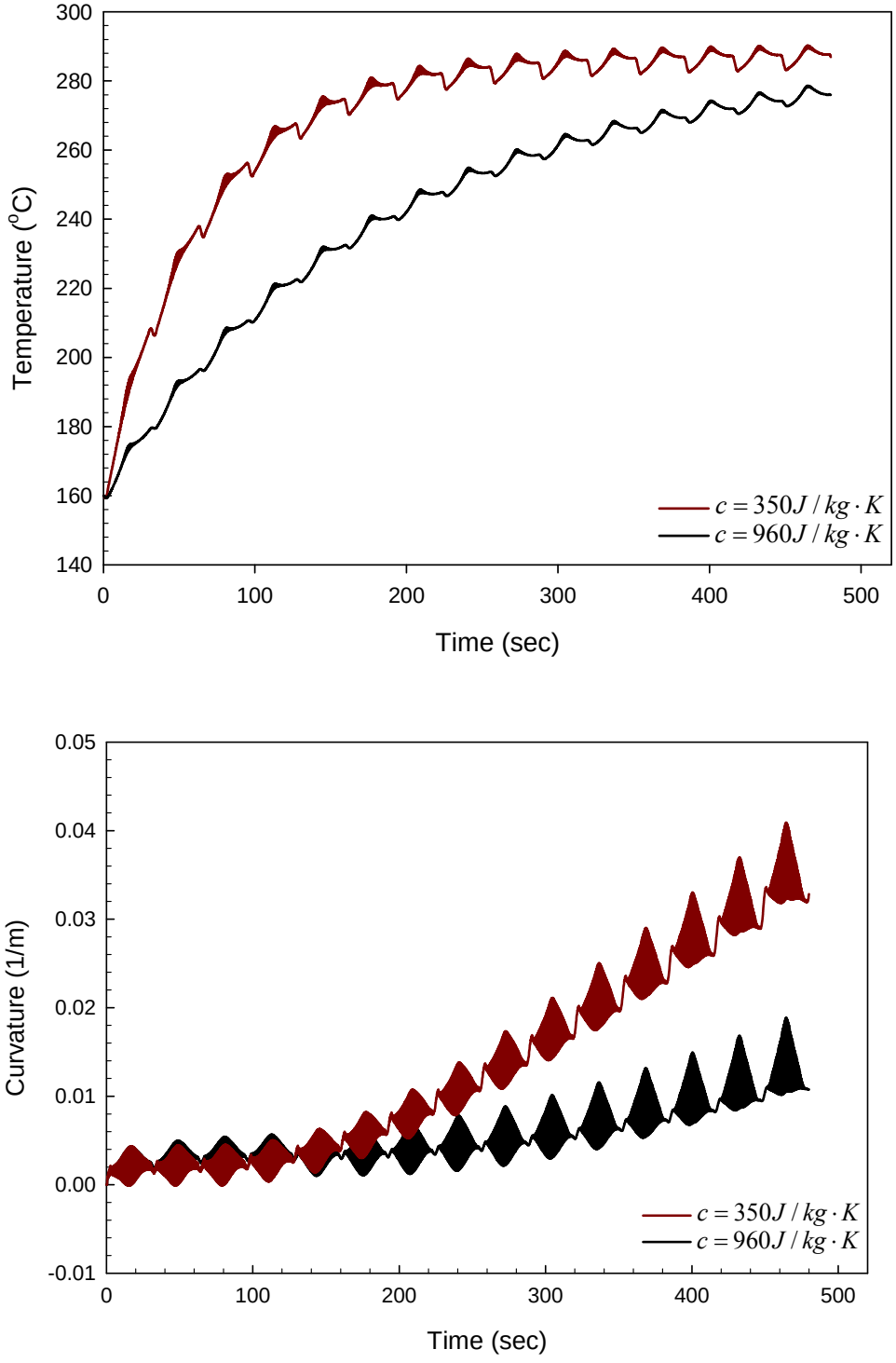

Figure 26. Deposition simulation with different value of specific heat of substrate.

Table 1. Basic parameters of specimens' simulations carried out to match the experiment. These values can be obtained directly through the experiment data except for the heat flux value in the last column.

Specimen	Feed Rate (g/min)	Raster Speed (mm/s)	Deposition Job Time (sec)	Thickness of Layer (mm)	Heat Flux (W/m^2)
R918	45	250	0.367	0.0449	300
R920	15	250	0.367	0.0168	260
R921	15	750	0.220	0.0056	182
R922	45	750	0.220	0.0166	210

Table 2. Thickness of path and steady state temperature of four specimen experiments. T_{st} Stands for the temperature achieved in steady state.

Raster Speed / Feed Rate	250 mm/s	750 mm/s
15 g/min	**R920** 16.8μm/pass, T_{st} = ~275C	**R921** 5.6μm/pass, T_{st} = ~200C
45 g/min	**R918** 44.9μm/pass, T_{st} = ~310C	**R922** 12.5μm/pass, T_{st} = ~225C